

2012

## Syntheses, Characterization, Density Functional Theory Calculations, and Activity of Tridentate SNS Zinc Pincer Complexes Based on Bis-Imidazole or Bis-Triazole Precursors

Follow this and additional works at: <https://digitalcommons.fairfield.edu/chemistry-facultypubs>

John R. Miecznikowski

Fairfield University, [imecznikowski@fairfield.edu](mailto:imecznikowski@fairfield.edu)

NOTICE: this is the author's version of a work that was accepted for publication in *Inorganica Chimica Acta*. Changes resulting from the publishing process, such as peer review, editing, corrections, structural formatting, and other quality control mechanisms may not be reflected in this document. Changes may have been made to this work since it was submitted for publication. A definitive version was subsequently published in *Inorganica Chimica Acta*, 2012, 387, 25-36. DOI:10.1016/j.ica.2011.12.047  
Lauren C. Keilich

### Peer Reviewed

*See next page for additional authors*

---

### Repository Citation

Miecznikowski, John R.; Lo, Wayne; Lynn, Matthew A.; Jain, Swapan S.; Keilich, Lauren C.; Kloczko, Nathan F.; O'Loughlin, Brianne E.; DiMarzio, A. P.; Foley, K. M.; Lisi, G. P.; Kwiecien, D. J.; Butrick, Elizabeth E.; Powers, E.; and Al-Abbasee, R., "Syntheses, Characterization, Density Functional Theory Calculations, and Activity of Tridentate SNS Zinc Pincer Complexes Based on Bis-Imidazole or Bis-Triazole Precursors" (2012). *Chemistry & Biochemistry Faculty Publications*. 14.

<https://digitalcommons.fairfield.edu/chemistry-facultypubs/14>

### Published Citation

Miecznikowski, J.R.; Lo, W.; Lynn, M.A.; Jain, S.; Keilich, L.C.; Kloczko, N.F.; O'Loughlin, B.E.; DiMarzio, A.P.; Foley, K.M.; Lisi, G.P.; Kwiecien, D.J.; Butrick, E.E.; Powers, E.; Al-Abbasee, R. "Syntheses, Characterization, Density Functional Theory Calculations, and Activity of Tridentate SNS Zinc Pincer Complexes Based on Bis-Imidazole or Bis-Triazole Precursors." *Inorganica Chimica Acta*, 2012, 387, 25-36.

This item has been accepted for inclusion in DigitalCommons@Fairfield by an authorized administrator of DigitalCommons@Fairfield. It is brought to you by DigitalCommons@Fairfield with permission from the rights-holder(s) and is protected by copyright and/or related rights. **You are free to use this item in any way that is permitted by the copyright and related rights legislation that applies to your use. For other uses, you need to obtain permission from the rights-holder(s) directly, unless additional rights are indicated by a Creative Commons license in the record and/or on the work itself.** For more information, please contact [digitalcommons@fairfield.edu](mailto:digitalcommons@fairfield.edu).

---

## Authors

John R. Miecznikowski, Wayne Lo, Matthew A. Lynn, Swapan S. Jain, Lauren C. Keilich, Nathan F. Kloczko, Brianne E. O'Loughlin, A. P. DiMarzio, K. M. Foley, G. P. Lisi, D. J. Kwiecien, Elizabeth E. Butrick, E. Powers, and R. Al-Abbasee

Syntheses, Characterization, Density Functional Theory Calculations, and  
Activity of Tridentate SNS Zinc Pincer Complexes  
Based on Bis-Imidazole or Bis-Triazole Precursors

John R. Miecznikowski<sup>a\*</sup>; Wayne Lo<sup>b</sup>; Matthew A. Lynn<sup>c</sup>; Swapan Jain<sup>d</sup>;  
Lauren C. Keilich<sup>a</sup>; Nathan F. Kloczko<sup>a</sup>; Brianne E. O'Loughlin<sup>a</sup>; Amanda P. DiMarzio<sup>a</sup>;  
Kathleen M. Foley<sup>a</sup>; George P. Lisi<sup>a</sup>; Daniel J. Kwiecien<sup>a</sup>; Elizabeth E. Butrick<sup>a</sup>; Erin  
Powers<sup>a</sup>, and Raed Al-Abbasee<sup>d</sup>

<sup>a</sup>Department of Chemistry and Biochemistry, Fairfield University, 1073 North Benson  
Road, Fairfield, CT 06824. U.S.A.

<sup>b</sup> Department of Chemistry, Boston College, 140 Commonwealth Avenue, Chestnut Hill,  
MA 02467. U.S.A.

<sup>c</sup>Department of Science and Mathematics, National Technical Institute for the Deaf,  
Rochester Institute of Technology, 52 Lomb Memorial Drive, Rochester, NY 14623.  
U.S.A.

<sup>d</sup> Department of Chemistry, Bard College, PO Box 5000, Annandale-on-Hudson, NY  
12504-5000. U.S.A.

\* Corresponding Author: Tel.: 1-(203) 254-4000 x 2125; Fax: 1-(203) 254-4034;  
Email: [jmiecznikowski@fairfield.edu](mailto:jmiecznikowski@fairfield.edu)

**Abstract:**

A series of tridentate pincer ligands, each possessing two sulfur- and one nitrogen-donor functionalities (SNS), based on bis-imidazole or bis-triazole salts were metallated with  $\text{ZnCl}_2$  to give new tridentate SNS pincer zinc(II) complexes  $[(\text{SNS})\text{ZnCl}]^+$ . The zinc complexes serve as models for the zinc active site in Liver Alcohol Dehydrogenase (LADH) and were characterized with single crystal X-ray diffraction,  $^1\text{H}$ ,  $^{13}\text{C}$ , and HSQC NMR spectroscopies, electrospray mass spectrometry, and elemental analysis. The zinc complexes feature SNS donor atoms and pseudotetrahedral geometry about the zinc center, as is seen for liver alcohol dehydrogenase. The bond lengths and bond angles of the zinc complexes correlate well to those in horse LADH. The SNS ligand precursors were characterized with  $^1\text{H}$ ,  $^{13}\text{C}$ , and HSQC NMR spectroscopies, elemental analysis, and cyclic voltammetry, and were found to be redox active. Gaussian calculations were performed and agree with the experimentally observed oxidation potentials for the pincer ligand precursors. The zinc complexes were screened for the reduction of electron-poor aldehydes in the presence of a hydrogen donor, 1-benzyl-1,4-dihydronicotinamide (BNAH), and it was determined that they enhance the reduction of electron-poor aldehydes. The SNS zinc pincer complexes with bis-triazole ligand precursors exhibit higher activity for the reduction of 4-nitrobenzaldehyde than do SNS zinc pincer complexes with bis-imidazole ligand precursors. Quantitative stoichiometric conversion was seen for the reduction of pyridine-2-carboxaldehyde via SNS zinc pincer complexes with either bis-imidazole or bis-triazole ligand precursors.

**Keywords:**

SNS pincer ligand  
Mononuclear Zn complexes  
X-ray crystallography  
Cyclic voltammetry  
Density functional theory calculations  
Aldehyde reductions

**1. Introduction:**

The synthesis and characterization of complexes that attempt to mimic natural catalytic behavior have furthered the understanding of the enzymatic activity of metalloenzyme sites [1]. Model complexes are low molecular mass systems that replicate the metalloenzyme in terms of structures, ligand donor atoms, and oxidation states [2]. Nature is used as a model for the design of highly active and efficient catalysts, and is also the inspiration behind the synthesis of each model complex in order to investigate structures and functions of enzymes.

Liver alcohol dehydrogenase (LADH) is a zinc metalloenzyme that catalyzes the oxidation of alcohols to aldehydes and ketones, and also catalyzes the reverse reaction, which is the reduction of a ketone or an aldehyde to an alcohol [1,3]. The crystal structure of horse LADH has been solved [4]. The resting enzyme includes one zinc(II) metal center, which is pseudo-tetrahedrally ligated with a labile water molecule and a so-called "SNS" ligand environment containing one N-histidine and two S-cysteine side chains. The nitrogen and sulfur atoms are provided by the histidine and cysteine residues of a single polypeptide chain [5]. Several LADH models have been previously reported with the same electron donor atoms as the metalloenzyme [6-13]. However, reactivity data was either not reported in some cases [14] or it was determined for zinc LADH model

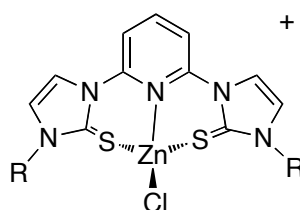
complexes possessing donor atoms that are different than those within the enzyme's active site [15].

In a continuous effort to understand the catalytic activity of metalloenzymes, we have chosen to model the structure and reactivity of the zinc active site in LADH using a new and unique family of robust SNS pincer ligands. First published in 1976, tridentate pincer ligands offer several advantages over monodentate ligands [16]. Primarily, tridentate pincer ligands offer favored metallation due to a less negative delta entropy of formation in comparison to monodentate ligands, which makes their metal complexes more stable [16]. Secondly, tridentate pincer ligands have been shown to inhibit dimerization of the metal complexes as a whole, a process that could possibly slow or inhibit catalytic activity [16, 17]. Thirdly, the conformational and electronic properties of tridentate ligands can be tuned by using different starting materials in their syntheses. Depending largely on the electron count of the metal center, tridentate pincer ligands can coordinate the metal atom in either a facial or meridional fashion [16, 17].

Pincer ligands have been utilized successfully in organometallic chemistry to prepare highly catalytically active and robust complexes [17]. The pincer ligand is an excellent system for use in modeling biological activity since the N-atom of pyridine, is  $sp^2$ -hybridized like that of histidine, and the thioimidazolyl S-donors have been reported by Parkin and Vahrenkamp to model thiol-derived ligands in bio-inspired zinc chemistry [18,19].

To the best of our knowledge, such tridentate pincer ligand systems have rarely been used in bio-inspired modeling chemistry. Our group has already had success in preparing tridentate SNS ligands that incorporate thione-substituted based imidazole functionalities

as well as zinc model complexes that contain these ligands [20]. The tridentate ligands used in these systems were relatively rigid as the pyridine and the imidazoles were directly bound to each other. Further, in an effort to understand the presence and sterics of ancillary alkyl groups on the ability of this model system to reduce aldehydes, the ligands were prepared with imidazolyl rings having R groups of various sizes as shown in Figure 1.



R = *i*Pr, neopentyl, *n*-butyl

**Figure 1:** Zinc-based SNS model complexes previously prepared by Miecznikowski *et al.* [20]

In our current work, we seek to further our understanding of the catalytic nature of the zinc complexes by tuning the structure of tridentate SNS-pincer ligands. Previously, we prepared somewhat rigid ligand systems through the use of 2,6-dibromopyridine as a ligand precursor. Here, we use the starting material 2,6-(dibromomethyl)pyridine to introduce a methylene linker into the pincer ligand, thereby allowing us to examine the effect of ligand flexibility on substrate binding toward the goal of better understanding the catalytic activity of LADH. In a similar vein, Crabtree and co-workers have shown that such a modification in Pd CNC-pincer complexes leads to improved catalytic activity in carbon-carbon bond formation reactions [21]. We expect to fine-tune further the electronic environment imparted by our ligand set through the use of imidazole- and triazole-based precursors in the preparation of the pincer ligand precursor as has been

shown previously by Crabtree and Miecznikowski [22]. Furthermore, sulfur-substituted triazoline systems (1,2,4-triazolinethiones) have been prepared by others, so we have adapted their synthetic protocol for use in our current work [23].

We therefore present here the syntheses, spectroscopic and electrochemical characterization, computational study, and activity screening of various tridentate SNS-pincer complexes of zinc in which the ligand set is modified through the placement of a methylene linker between its pyridinyl and imidazolyl or triazolyl segments.

## **2. Experimental:**

### ***2.1 General Procedures:***

All reagents used are commercially available and were used as received. Isopropyl imidazole, neopentyl imidazole, 1-isopropyl triazole, 1-*n*-butyl triazole, 1-neopentyl triazole, 2,6-bis{[(*n*-butyl)-*N'*-methylene]imidazole}pyridine bromide, were prepared as reported previously [24-27]. BNA<sup>+</sup> and BNAH were prepared as reported previously [28].

NMR spectra were recorded at 25 °C on a Bruker Avance 300 MHz NMR spectrometer. Spectra were referred to the solvent residual peak. Electrospray mass spectrometry was performed on a Micromass ZQ instrument or a Varian LC-MS instrument using nitrogen as the drying and nebulizing gas. Cyclic voltammetry experiments were performed using a Cypress Electroanalytical System with a silver wire reference electrode, a glassy carbon working electrode, and a platinum counter electrode. The supporting electrolyte for the cyclic voltammetry experiments was tetra-*N*-butylammonium tetrafluoroborate. The ferrocenium/ferrocene couple was used as an

internal reference; reduction potential values were corrected by assigning the ferrocenium/ferrocene couple to 0.40 V versus SCE. When an inert atmosphere was needed, a M-Braun inert atmosphere glove box and standard Schlenk techniques were used with thoroughly degassed solvents. IR spectra were collected using a Thermo Nicolet AVATAR 380-FT-IR with a SMART SPECULATR reflectance adaptor. C, H, N elemental analyses were performed by Atlantic Microlab Inc. (Norcross, GA).

## ***2.2 Crystallographic Analyses:***

Crystals of **1**, **3**, **5b**, and **6** were mounted on a glass fiber or loop and placed in a -80 °C nitrogen stream on a Bruker diffractometer equipped with a Smart CCD at Boston College (Chestnut Hill, MA). Crystallographic data were collected using graphite monochromated 0.71073 Å Mo-K $\alpha$  radiation and integrated and corrected for absorption using the Bruker SAINTPLUS software package [29]. The structures were solved using direct methods and refined using least-square methods on F-squared [30]. All other pertinent crystallographic details such as h, k, l ranges, 2 $\theta$  ranges, and R-factors can be found in Table 1.

**Table 1.** Crystal and Structure Refinement Data for **1**, **3**, **5b**, and **6**

	R = <i>i</i> Pr ( <b>1</b> )	R = <i>n</i> Bu ( <b>3</b> )	R = <i>Np</i> ( <b>5b</b> )	R = <i>n</i> Bu ( <b>6</b> )
Formula	C <sub>42</sub> H <sub>55</sub> Cl <sub>6</sub> N <sub>12</sub> S <sub>4</sub> Zn <sub>3</sub>	C <sub>42</sub> H <sub>56</sub> Cl <sub>6</sub> N <sub>10</sub> S <sub>4</sub> Zn <sub>3</sub>	C <sub>21</sub> H <sub>31</sub> N <sub>7</sub> S <sub>2</sub>	C <sub>38</sub> H <sub>54</sub> Cl <sub>6</sub> N <sub>14</sub> S <sub>4</sub> Zn <sub>4</sub>
FW (g/mol)	1265.02	1238.02	445.65	1380.33
Temperature (K)	193(2)	193(2)	193(2)	193(2)
Wavelength (Å)	0.71073	0.71073	0.71073	0.71073
Crystal System	Triclinic	Monoclinic	Triclinic	Monoclinic
Space Group	P-1	P2(1)/c	P2(1)/c	P2(1)/c
a (Å)	7.0010(19)	20.2931(8)	20.655(3)	23.7884(13)
b (Å)	19.310(5)	21.6238(9)	11.2349(17)	11.0040(6)
c (Å)	21.789(6)	13.2096(6)	10.6710(16)	21.1704(11)
α (°)	70.872(8)	90	90	90
β (°)	80.971(5)	107.064(2)	103.218(3)	99.770(3)
γ (°)	79.577(5)	90	90	90
Volume (Å) <sup>3</sup>	2722.0(13)	5541.4(4)	2410.6(6)	5461.4(5)
Z	4	8	4	8
r (calc) (g/cm <sup>3</sup> )	1.543	1.484	1.228	1.679
Abs (mm <sup>-1</sup> )	1.802	1.768	0.243	2.324
F(000)	1294	2536	952	2800
Crystal Size (mm <sup>3</sup> )	0.20 x 0.10 x 0.10	0.10 x 0.08 x 0.08	0.20 x 0.20 x 0.08	0.08 x 0.06 x 0.05
Theta Range (°)	0.99 to 28.46	1.87 to 22.50	1.01 to 28.26	1.74 to 26.31
Refl/Uniq	43409/13420	31379/7243	35218/5914	48222/11044
R(int)	0.0780	0.0713	0.0659	0.0799
Abs Correction	None	None	None	None
Max./Min	0.8403/0.7145	0.8715/0.8430	0.9809/0.95 31	0.8926/0.8359
Ref Method	Full Matrix least squares on F <sup>2</sup>	Full Matrix least squares on F <sup>2</sup>	Full Matrix least squares on F <sup>2</sup>	Full Matrix least squares on F <sup>2</sup>
Data / restr / par	13420 / 0 / 614	7243/0/562	5914 / 0 / 277	11044/ 0/ 639
GOF on	0.868	1.018	0.627	0.971

F <sup>2</sup>				
R1	0.0450	0.0913	0.0488	0.0473
indices (I>2s)				
wR2	0.0911	0.2159	0.1357	0.0822
Peak/hole (e/Å <sup>-3</sup> )	0.751 and -0.765	2.055 and -2.142	0.440 and - 0.256	0.869 and -0.673

### 2.3 Reactivity:

In a typical reaction, 0.1 mmol of 4-nitrobenzaldehyde (or pyridine 2-carboxaldehyde), 0.2 mmol of BNAH, and 0.1 mmol of the zinc complex or 0.2 mmol ZnCl<sub>2</sub> were dissolved in 3 mL of CDCl<sub>3</sub>. The reaction was heated at reflux. Aliquots of the reaction were taken at certain times and analyzed using <sup>1</sup>H NMR spectroscopy. All data are averages of at least two runs.

### 2.4 Gaussian Calculations:

Gaussian 03 was used to perform single-point calculations and DFT geometry optimizations using the B3LYP hybrid functional with 6-31G\* basis sets as provided with the software [31]. Calculations were performed on the ligands alone with R = Me in all cases. The structures of the ligands were first optimized in the gas phase as neutral and as cationic species under the C<sub>s</sub> and C<sub>2</sub> point groups. Frequency analysis was performed on the optimized structures to determine whether or not they represented true minima. Small imaginary frequencies on the order of ~ -10 cm<sup>-1</sup> that are not indicative of transition-state structures were found only for the neutral structures of the thiotriazole systems having C<sub>s</sub> symmetry. Single-point SCRF calculations using DMSO via the CPCM solvent model were then performed using the “radii=uff” and “nosymm cav”

directives. Oxidation potentials were computed by finding the difference in the total free energies in solution for the neutral and cationic species. These  $\Delta G$  values were then referenced to the absolute SCE potential in DMSO by subtracting 3.83V (the established correction to SHE in DMSO) and 0.241 V (the difference between SHE and SCE) [32].

## 2.5 Syntheses:

### Syntheses of ligand precursor bromide salts.

As an example, a detailed description for the synthesis of **1a** is given. Detailed descriptions for the preparation of all the ligand precursor bromide salts are given in supporting information.

#### 2.5.1 Synthesis of 2,6-bis(N-isopropyl-N'-methyleneimidazole)pyridine bromide, (C<sub>19</sub>H<sub>27</sub>N<sub>5</sub>Br<sub>2</sub>): [1a]

In a 100 mL round-bottom flask, 1.53g (5.78 mmol) 2,6-bis(bromomethyl)pyridine was combined with 1.99 g (18.0 mmol) 1-isopropyl-1,3-imidazole and dissolved in 10mL of 1,4-dioxane. The solution was stirred at reflux overnight during which time, a brown precipitate formed. The solid was collected with a Buchner funnel and washed with diethyl ether (3x, 30 mL each). This solid was then taken up in methanol (10 mL) and precipitated in diethyl ether. This solution was vacuum filtered and the solid product was washed with diethyl ether (3x, 30 mL each). Yield: 2.42 g (86.3%). Anal. Calc. for C<sub>19</sub>H<sub>27</sub>Br<sub>2</sub>N<sub>5</sub> (485.26): C, 47.03; H, 5.61; N, 14.43. Found: C, 46.95; H, 5.74; N, 14.19.

$^1\text{H}$  NMR (DMSO- $d_6$ , 300 MHz)  $\delta$  9.47 (s, 2H, imidazole, CH), 7.98 (m, 3H, pyridine CH, and imidazole CH), 7.78 (d ( $^3J = 1.8$  Hz), 2H, imidazole CH), 7.49 (d ( $^3J = 7.5$  Hz), 2H, pyridine CH), 5.56 (s, 4H,  $\text{CH}_2$ ), 4.71 (m, 2H, isopropyl CH), 1.49 (d ( $^3J = 6.9$  Hz), 12H,  $\text{CH}_3$ ).  $^{13}\text{C}$   $\{^1\text{H}\}$  NMR (DMSO- $d_6$ , 75 MHz),  $\delta$  153.65 (imidazole NCHN), 138.88 (pyridine CH), 135.50 (pyridine  $\text{C}_{\text{ipso}}$ ), 123.30 (imidazole CH), 122.22 (pyridine CH), 120.45 (imidazole CH), 52.69 ( $\text{CH}_2$ ), 52.30 (isopropyl CH), 22.32 (isopropyl  $\text{CH}_3$ ).

### 2.5.2 Synthesis of 2,6-bis(N-neopentyl-N'-methyleneimidazole)pyridine bromide, ( $\text{C}_{23}\text{H}_{35}\text{N}_5\text{Br}_2$ ): [2a]

Yield: 3.40 g (quantitative). Anal. Calc. for  $\text{C}_{23}\text{H}_{35}\text{Br}_2\text{N}_5 \cdot \text{H}_2\text{O}$  (559.38): C, 49.38; H, 6.67; N, 12.52. Found: C, 49.07; H, 6.67; N, 12.34.

$^1\text{H}$  NMR (DMSO- $d_6$ , 300 MHz)  $\delta$  9.33 (s, 2H, imidazole, CH), 7.99 (m, 1H, pyridine CH), 7.77 (d ( $^3J = 1.5$  Hz), 4H, imidazole CH), 7.46 (d ( $^3J = 7.8$  Hz), 2H, pyridine CH), 5.59 (s, 4H,  $\text{CH}_2$ ), 4.01 (s, 4H, neopentyl  $\text{CH}_2$ ), 0.92 (s, 18H, neopentyl  $\text{CH}_3$ ).  $^{13}\text{C}$   $\{^1\text{H}\}$  NMR (DMSO- $d_6$ , 75 MHz),  $\delta$  153.71 (pyridine  $\text{C}_{\text{ipso}}$ ), 138.90 (pyridine CH), 137.41 (imidazole CH), 123.77 (imidazole CH), 122.66 (imidazole CH), 122.02 (pyridine CH), 59.45 (neopentyl  $\text{CH}_2$ ), 52.71 ( $\text{CH}_2$ ), 31.93 (neopentyl  $\text{C}(\text{CH}_3)_3$ ), 26.63 (neopentyl  $\text{CH}_3$ ).

### 2.5.3 Synthesis of 2,6-bis(N-isopropyl-N'-methylenetriazole)pyridine bromide ( $\text{C}_{17}\text{H}_{25}\text{N}_7\text{Br}_2$ ), [4a]:

Yield: 1.87g (94 %). Anal. Calc. for  $\text{C}_{17}\text{H}_{25}\text{Br}_2\text{N}_7$  (487.24): C, 41.91; H, 5.17; N, 20.12. Found: C, 42.01; H, 5.19; N, 19.93.

$^1\text{H}$  NMR (DMSO- $d_6$ , 300 MHz)  $\delta$  10.37 (s, 2H, triazole CH), 9.24 (s, 2H, triazole CH), 8.01 (m, 1H, pyridine CH), 7.62 (d ( $^3J = 7.8$  Hz), 2H, pyridine CH), 5.69 (s, 4H,  $\text{CH}_2$ ), 4.87 (m, 2H, isopropyl CH), 1.56 (d ( $^3J = 6.0$  Hz), 12H, isopropyl  $\text{CH}_3$ ).  $^{13}\text{C}$   $\{^1\text{H}\}$  NMR (DMSO- $d_6$ , 75 MHz),  $\delta$  152.28 (triazole NCHN), 145.17 (triazole CH), 141.79 (pyridine CH), 138.84 (pyridine  $\text{C}_{\text{ipso}}$ ), 122.51 (pyridine CH), 55.16 ( $\text{CH}_2$ ), 50.69 (isopropyl CH), 21.15 (isopropyl  $\text{CH}_3$ ).

#### 2.5.4 Synthesis of 2,6-bis(N-neopentyl-N'-methylenetriazole)pyridine bromide

**( $\text{C}_{21}\text{H}_{33}\text{N}_7\text{Br}_2$ ) [5a]:**

Yield: 2.05g (quantitative). Anal. Calc. for  $\text{C}_{21}\text{H}_{33}\text{N}_7\text{Br}_2 \cdot 0.5 \text{H}_2\text{O}$  (543.34): C, 45.66; H, 6.20; N, 17.75. Found: C, 45.48; H, 6.18; N, 17.69.

$^1\text{H}$  NMR (DMSO- $d_6$ , 300 MHz)  $\delta$  10.43 (s, 2H, triazole, CH), 9.34 (s, 2H, triazole, CH), 8.04 (m, 1H, pyridine CH), 7.63 (d ( $^3J = 7.8$  Hz), 2H, pyridine CH), 5.76 (s, 4H,  $\text{CH}_2$ ), 4.31 (s, 4H,  $\text{CH}_2$ ), 0.96 (s, 18H,  $\text{CH}_3$ ).  $^{13}\text{C}$   $\{^1\text{H}\}$  NMR (DMSO- $d_6$ , 75 MHz),  $\delta$  152.37 (pyridine  $\text{C}_{\text{ipso}}$ ), 145.01 (triazole CH), 143.61 (triazole CH), 138.94 (pyridine CH), 122.52 (pyridine CH), 61.92 ( $\text{CH}_2$ ), 50.89 ( $\text{CH}_2$ ), 32.15 (neopentyl  $\text{C}(\text{CH}_3)_3$ ), 26.72 (neopentyl  $\text{C}(\text{CH}_3)_3$ ).

#### 2.5.5 Synthesis of 2,6-bis[N-(*n*-butyl)-N'-methylenetriazole]pyridine bromide

**( $\text{C}_{21}\text{H}_{31}\text{N}_5\text{Br}_2$ ) [6a]:**

Yield: 1.11 g (quantitative). Anal. Calc. for  $\text{C}_{19}\text{H}_{29}\text{Br}_2\text{N}_7 \cdot 2\text{H}_2\text{O} \cdot \text{CH}_3\text{OH}$  (515.29): C, 42.22, H, 6.58, N, 16.41. Found: C, 41.82; H, 6.09; N, 15.83.

$^1\text{H}$  NMR (DMSO- $d_6$ , 300 MHz)  $\delta$  10.30 (s, 2H, triazole, CH), 9.23 (s, 2H, triazole CH), 8.03 (m, 1H, pyridine CH), 7.61 (d ( $^3J = 7.5$  Hz), 2H, pyridine CH), 5.70 (s, 4H, CH<sub>2</sub>), 4.44 (t ( $^3J = 7.2$  Hz), 4H, n-butyl CH<sub>2</sub>), 1.87 (m, 4H, n-butyl CH<sub>2</sub>), 1.33 (m, 4H, n-butyl CH<sub>2</sub>), 0.947 (m, 6H, n-butyl CH<sub>3</sub>).  $^{13}\text{C}$  { $^1\text{H}$ } NMR (DMSO- $d_6$ , 75 MHz),  $\delta$  152.30 (pyridine CH), 145.31 (pyridine CH), 142.99 (triazole CH), 142.53 (triazole CH), 122.42 (pyridine C<sub>ipso</sub>), 51.40 (CH<sub>2</sub>), 48.57 (n-butyl CH<sub>2</sub>), 30.01 (n-butyl CH<sub>2</sub>), 18.75 (n-butyl CH<sub>2</sub>), 13.28 (n-butyl CH<sub>3</sub>).

### Syntheses of Bis-thione ligand precursors:

As an example, a detailed description for the synthesis of **1b** is given. Detailed descriptions for the preparation of all the bis-thione ligand precursors are given in supporting information.

#### 2.5.6 Synthesis of 2,6-bis(N-isopropyl-N'-methyleneimidazole-2-thione)pyridine (C<sub>19</sub>H<sub>25</sub>N<sub>5</sub>S<sub>2</sub>) [**1b**]

In a round-bottom flask, 0.24 g (0.50 mmol) of **1a** was added to 0.12 g (1.5 mmol) of sodium acetate. Acetonitrile (20 mL) was added to the solid mixture. The reaction mixture was heated at reflux for a half hour during which, the solids dissolved in the acetonitrile. To this solution, 0.34 g (11 mmol) of S<sub>8</sub> and the mixture was heated at reflux for seven days. Afterwards, the undissolved solid was filtered out of the mother liquor. The solvent was evaporated off under reduced pressure. The resulting product was oily. The product was dissolved in dichloromethane and was filtered to remove excess sodium acetate. The solvent was removed under reduced pressure. Yield: 0.13 g (70. %). Anal. Calc. C<sub>19</sub>H<sub>25</sub>N<sub>5</sub>S<sub>2</sub> • 0.5H<sub>2</sub>O (387.57): C, 57.54; H, 6.61; N, 17.66. Found: C, 57.32; H, 6.37; N, 17.45.

$^1\text{H}$  NMR (DMSO- $d_6$ , 300 MHz)  $\delta$  7.73 (t ( $^3J = 7.8$  Hz), 1H, pyridine, CH), 7.31 (d ( $^3J = 2.7$  Hz), 2H, imidazole CH), 7.22 (d ( $^3J = 2.4$  Hz), 2H, imidazole CH), 6.91 (d ( $^3J = 7.8$  Hz), 2H, pyridine CH), 5.30 (s, 4H,  $\text{CH}_2$ ), 4.89 (m, 2H, isopropyl CH), 1.32 (d ( $^3J = 6.9$  Hz), 12H,  $\text{CH}_3$ ).  $^{13}\text{C}\{^1\text{H}\}$  NMR (DMSO- $d_6$ , 75 MHz),  $\delta$  160.92 (C=S), 155.80 (pyridine  $\text{C}_{\text{ipso}}$ ), 137.80 (pyridine CH), 120.08 (pyridine CH), 118.39 (imidazole CH), 114.03 (imidazole CH), 51.15 ( $\text{CH}_2$ ), 48.41 (isopropyl CH), 21.14 (isopropyl  $\text{CH}_3$ ). Selected IR bands (reflectance):  $\nu_{\text{max}}/\text{cm}^{-1}$  1129 (C=S).

### 2.5.7 Synthesis of 2,6-bis(N-neopentyl-N'-methyleneimidazole-2-thione)pyridine ( $\text{C}_{23}\text{H}_{33}\text{N}_5\text{S}_2$ ), [2b]:

Yield: 0.26 g (60. %). Anal. Calc.  $\text{C}_{23}\text{H}_{33}\text{N}_5\text{S}_2 \cdot 3\text{H}_2\text{O}$  (443.67): C, 58.69; H, 7.71; N, 14.88. Found: C, 58.86; H, 7.09; N, 14.79.

$^1\text{H}$  NMR (DMSO- $d_6$ , 300 MHz)  $\delta$  7.30 (m, 1H, pyridine, CH), 7.22 (d ( $^3J = 2.1$  Hz), 2H, imidazole CH), 7.16 (d ( $^3J = 2.1$  Hz), 2H, imidazole CH), 6.86 (d ( $^3J = 7.8$  Hz), 2H, pyridine CH), 5.32 (s, 4H,  $\text{CH}_2$  linker), 3.92 (s, 4H, neopentyl  $\text{CH}_2$ ), 0.96 (s, 18H, neopentyl  $\text{CH}_3$ ),  $^{13}\text{C}\{^1\text{H}\}$  NMR (DMSO- $d_6$ , 75 MHz),  $\delta$  163.54 (C=S), 155.93 (pyridine  $\text{C}_{\text{ipso}}$ ), 137.74 (pyridine CH), 119.68 (pyridine CH), 118.81 (imidazole CH), 117.55 (imidazole CH), 57.03 (neopentyl  $\text{CH}_2$ ), 51.63 ( $\text{CH}_2$  linker), 33.63 (neopentyl  $\text{C}(\text{CCH}_3)_3$ ), 27.82 (neopentyl  $\text{CH}_3$ ). Selected IR bands (reflectance):  $\nu_{\text{max}}/\text{cm}^{-1}$  1128 (C=S).

### 2.5.8 Synthesis of 2,6-bis[N-(*n*-butyl)-N'-methyleneimidazole-2-thione]pyridine ( $\text{C}_{21}\text{H}_{29}\text{N}_5\text{S}_2$ ) [3b]

Yield: 0.10 g (23. %). Anal. Calc. for  $\text{C}_{21}\text{H}_{29}\text{N}_5\text{S}_2 \cdot \text{H}_2\text{O}$  (415.62): C, 58.17; H, 7.21; N, 16.15. Found: C, 57.60; H, 6.66; N, 15.84.

$^1\text{H}$  NMR (DMSO- $d_6$ , 300 MHz)  $\delta$  7.73 (m, 1H, pyridine, CH), 7.21 (d ( $^3J$  = 2.4 Hz), 2H, imidazole CH), 7.19 (d ( $^3J$  = 2.4 Hz), 2H, imidazole CH), 6.91 (d ( $^3J$  = 7.8 Hz), 2H, pyridine CH), 5.29 (s, 4H,  $\text{CH}_2$  linker), 3.98 (t ( $^3J$  = 7.2 Hz), 4H, butyl  $\text{CH}_2$ ), 1.69 (m, 4H, butyl  $\text{CH}_2$ ), 1.28 (m, 4H, butyl  $\text{CH}_2$ ), 0.94 (t ( $^3J$  = 7.2 Hz), 6H, butyl  $\text{CH}_3$ ),  $^{13}\text{C}$  { $^1\text{H}$ } NMR (DMSO- $d_6$ , 75 MHz),  $\delta$  161.78 (C=S), 155.83 (pyridine  $\text{C}_{\text{ipso}}$ ), 137.78 (pyridine CH), 119.97 (pyridine CH), 117.93 (imidazole CH), 117.64 (imidazole CH), 51.35 ( $\text{CH}_2$  linker), 46.65 (butyl  $\text{CH}_2$ ), 30.93 (butyl  $\text{CH}_2$ ), 22.04 (butyl  $\text{CH}_2$ ), 13.54 (butyl  $\text{CH}_3$ ). Selected IR bands (reflectance):  $\nu_{\text{max}}/\text{cm}^{-1}$  1129 (C=S).

### 2.5.9 Synthesis of 2,6-bis(N-isopropyl-N'-methylenetriazole-2-thione)pyridine

#### ( $\text{C}_{17}\text{H}_{23}\text{N}_7\text{S}_2$ ) [4b]

Yield: 0.31 g (78.%). Anal. Calc. for  $\text{C}_{17}\text{H}_{23}\text{N}_7\text{S}_2 \cdot 0.5\text{H}_2\text{O}$  (389.54): C, 51.23; H, 6.07; N, 24.60. Found: C, 51.36; H, 5.92; N, 24.43.

$^1\text{H}$  NMR (DMSO- $d_6$ , 300 MHz)  $\delta$  8.46 (s, 2H, triazole CH), 7.82 (t ( $^3J$  = 7.8 Hz), 1H, pyridine CH), 7.26 (d ( $^3J$  = 7.8 Hz), 2H, pyridine CH), 5.28 (s, 4H,  $\text{CH}_2$ ), 4.92 (m, 2H, isopropyl CH), 1.35 (d ( $^3J$  = 6.6 Hz), 12H, isopropyl  $\text{CH}_3$ ).  $^{13}\text{C}$  { $^1\text{H}$ } NMR (DMSO- $d_6$ , 75 MHz),  $\delta$  164.02 (C=S), 154.12 (pyridine  $\text{C}_{\text{ipso}}$ ), 141.33 (triazole CH), 137.95 (pyridine CH), 121.10 (pyridine CH), 49.76 (isopropyl CH), 48.85 ( $\text{CH}_2$ ), 20.50 (isopropyl  $\text{CH}_3$ ). Selected IR bands (reflectance):  $\nu_{\text{max}}/\text{cm}^{-1}$  1158 (C=S).

### 2.5.10 Synthesis of 2,6-bis(N-neopentyl-N'-methylenetriazole-2-thione)pyridine

#### ( $\text{C}_{21}\text{H}_{31}\text{N}_7\text{S}_2$ ), [5b]:

Yield 0.42 g (82 %). Off-white crystals of **5b** that were suitable for X-ray diffraction were grown by allowing diethyl ether to slowly diffuse into a solution of **5b** in

acetonitrile. Anal. Calc. for  $C_{21}H_{31}N_7S_2 \cdot 0.5 CH_2Cl_2$ : C, 52.90; H, 6.61; N, 20.09.

Found: C, 52.54, H, 6.45, N, 20.40.

$^1H$  NMR (DMSO- $d_6$ , 300 MHz)  $\delta$  8.50 (s, 2H, triazole CH), 7.82 (m, 1H, pyridine CH), 7.21 (d ( $^3J = 7.8$  Hz), 2H, pyridine CH), 5.29 (s, 4H,  $CH_2$ ), 3.99 (s, 4H, neopentyl  $CH_2$ ), 0.91 (s, 18H, neopentyl  $CH_3$ ).  $^{13}C\{^1H\}$  NMR (DMSO- $d_6$ , 75 MHz),  $\delta$  167.66 (C=S), 155.08 (pyridine  $C_{ipso}$ ), 142.00 (triazole CH), 138.84 (pyridine CH), 121.69 (pyridine CH), 59.23 (neopentyl  $CH_2$  linker), 50.21 ( $CH_2$  linker) 34.51 ( $C(CH_3)_3$ ), 28.64 ( $C(CH_3)_3$ ). Selected IR bands (reflectance):  $\nu_{max}/cm^{-1}$  1144 (C=S).

### 2.5.11 Synthesis of 2,6-bis[N-(*n*-butyl)-N'-methylenetriazole-2-thione]pyridine

( $C_{19}H_{29}N_7S_2Br_2$ ) [6b]

Yield 0.17 g (46 %). Anal. Calc. for  $C_{19}H_{27}N_7S_2 \cdot 0.5 H_2O$  (417.59): C, 53.49; H, 6.62; N, 22.98. Found: C, 53.45, H, 6.55, N, 22.13.

$^1H$  NMR (DMSO- $d_6$ , 300 MHz)  $\delta$  8.47 (s, 2H, triazole CH), 7.80 (m, 1H, pyridine CH), 7.24 (d ( $^3J = 2.4$  Hz), 2H, pyridine CH), 7.23 (d ( $^3J = 2.7$  Hz), 2H, pyridine CH), 5.27 (s, 4H,  $CH_2$ ), 4.11 (t 7.24 (d ( $^3J = 4.8$  Hz), 2H, pyridine CH), 4H, *n*-butyl  $CH_2$ ), 1.74 (m, 4H, *n*-butyl  $CH_2$ ), 1.28 (m, 4H, *n*-butyl  $CH_2$ ), 0.900 (t ( $^3J = 4.8$  Hz), 6H, *n*-butyl  $CH_3$ ).  $^{13}C\{^1H\}$  NMR (DMSO- $d_6$ , 75 MHz),  $\delta$  165.10 (C=S), 154.09 (pyridine  $C_{ipso}$ ), 141.35 (triazole CH), 137.95 (pyridine CH), 120.94 (pyridine CH), 49.05 ( $CH_2$  linker), 47.99 (*n*-butyl  $CH_2$ ), 29.56 (*n*-butyl  $CH_2$ ), 19.04 (*n*-butyl  $CH_2$ ), 13.44 (*n*-butyl  $CH_3$ ). Selected IR bands (reflectance):  $\nu_{max}/cm^{-1}$  1149 (C=S).

### Syntheses of Zinc Complexes:

As an example, a detailed description for the synthesis of **1** is given. Detailed descriptions for the preparation of all the zinc complexes are given in supporting information.

**2.5.12 Synthesis of chloro-( $\eta^3$ -S,S,N)-[2,6-bis(N-isopropyl-N'-methyleneimidazole-2-thione)pyridine]zinc (II) tetrachlorozincate [C<sub>42</sub>H<sub>55</sub>Cl<sub>2</sub>N<sub>12</sub>S<sub>4</sub>Zn<sub>2</sub>][ZnCl<sub>4</sub>] [1]**

In a round-bottom flask, 0.13 g (0.34 mmol) of **1b** was combined with 0.098 g (0.72 mmol) of ZnCl<sub>2</sub> and dissolved in 10 mL of dichloromethane. The solution mixture was refluxed for 20 h. After this time, the solvent was removed under reduced pressure. Yield: 0.22 g (quantitative). White single crystals for X-ray diffraction were grown by a slow vapor diffusion of diethyl ether into an acetonitrile solution containing the zinc complex. Anal. Calc. for C<sub>19</sub>H<sub>27</sub>Cl<sub>4</sub>N<sub>5</sub>OS<sub>2</sub>Zn<sub>2</sub> (678.15): C, 33.65; H, 4.01; N, 10.33. Found: C, 33.58, H, 3.95, N, 10.54.

<sup>1</sup>H NMR (DMSO-d<sub>6</sub>, 300 MHz)  $\delta$  7.73 (m, 1H, pyridine CH), 7.31 (d (<sup>3</sup>J = 2.7 Hz), 2H, imidazole CH), 7.22 (d (<sup>3</sup>J = 2.4 Hz), 2H, imidazole CH), 6.90 (d (<sup>3</sup>J = 7.5 Hz), 2H, pyridine CH), 5.30 (s, 4H, CH<sub>2</sub>), 4.88 (m, 2H, isopropyl CH) 1.30 (d (<sup>3</sup>J = 6.6 Hz), 12H, isopropyl CH<sub>3</sub>). <sup>13</sup>C{<sup>1</sup>H} NMR (DMSO-d<sub>6</sub>, 75 MHz),  $\delta$  160.88 (C=S), 155.83 (pyridine C<sub>ipso</sub>), 137.85 (pyridine CH), 120.10 (pyridine CH), 118.45 (imidazole CH), 114.09 (imidazole CH), 51.18 (CH<sub>2</sub>), 48.45 (isopropyl CH), 21.30 (isopropyl CH<sub>3</sub>).

<sup>1</sup>H NMR (MeOH-d<sub>4</sub>, 300 MHz)  $\delta$  7.91 (t (<sup>3</sup>J = 7.8 Hz), 1H, pyridine CH), 7.45 (d (<sup>3</sup>J = 7.8 Hz), 2H, pyridine CH), 7.32 (m, 4H, imidazole CH), 5.54 (s, 4H, CH<sub>2</sub>), 4.97 (m, 2H, isopropyl CH) 1.40 (d (<sup>3</sup>J = 4.2 Hz), 12H, isopropyl CH<sub>3</sub>).

**2.5.13 Synthesis of chloro-( $\eta^3$ -S,S,N)-[2,6-bis(N-neopentyl-N'-methyleneimidazole-2-thione)pyridine]zinc (II) aquatrichlorozincate [C<sub>23</sub>H<sub>33</sub>N<sub>5</sub>S<sub>2</sub>ClZn][ZnCl<sub>3</sub>(OH<sub>2</sub>)] [2]**

Yield: 0.30 g (quantitative). The white product was purified dissolving the complex into acetonitrile and allowing diethyl ether vapor to diffuse in to the acetonitrile solution slowly. Anal. Calc. for C<sub>23</sub>H<sub>35</sub>Cl<sub>4</sub>N<sub>5</sub>OS<sub>2</sub>Zn<sub>2</sub> • 2 H<sub>2</sub>O (734.26): C, 35.86; H, 5.10; N, 9.09. Found: C, 35.60, H, 4.89, N, 8.99.

<sup>1</sup>H NMR (DMSO-d<sub>6</sub>, 300 MHz)  $\delta$  7.73 (m, 1H, pyridine CH), 7.21 (d (<sup>3</sup>J = 2.4 Hz), 2H, imidazole CH), 7.15 (d (<sup>3</sup>J = 2.4 Hz), 2H, imidazole CH), 6.84 (d (<sup>3</sup>J = 7.8 Hz), 2H, pyridine CH), 5.31 (s, 4H, CH<sub>2</sub>), 3.91 (s, 4H, CH<sub>2</sub>), 0.95 (s, 18H, CH<sub>3</sub>). <sup>13</sup>C {<sup>1</sup>H} NMR (DMSO-d<sub>6</sub>, 75 MHz),  $\delta$  163.70 (C=S), 156.01 (pyridine C<sub>ipso</sub>), 137.70 (pyridine CH), 119.85 (pyridine CH), 118.83 (imidazole CH), 117.57 (imidazole CH), 57.04 (neopentyl CH<sub>2</sub>), 51.64 (CH<sub>2</sub>), 33.64 (neopentyl C(CH<sub>3</sub>)<sub>3</sub>), 27.83 (neopentyl CH<sub>3</sub>).

<sup>1</sup>H NMR (MeOH-d<sub>4</sub>, 300 MHz)  $\delta$  7.90 (t (<sup>3</sup>J = 7.8 Hz), 1H, pyridine CH), 7.42 (d (<sup>3</sup>J = 7.5 Hz), 2H, pyridine CH), 7.26 (AB doublet (<sup>3</sup>J = 1.8 Hz), 2H, imidazole CH), 7.18 (AB doublet (<sup>3</sup>J = 1.8 Hz), 2H, imidazole CH), 5.60 (s, 4H, CH<sub>2</sub>), 4.01 (s, 4H, CH<sub>2</sub>), 1.01 (s, 18H, CH<sub>3</sub>).

**2.5.14 Synthesis of chloro-( $\eta^3$ -S,S,N)-{2,6-bis[N-(*n*-butyl)-N'-methyleneimidazole-2-thione]pyridine}zinc (II) tetrachlorozincate [C<sub>42</sub>H<sub>56</sub>Cl<sub>2</sub>N<sub>10</sub>S<sub>4</sub>Zn<sub>2</sub>][ZnCl<sub>4</sub>] [3]**

Yield: 0.11 g (quantitative). Off-white single crystals for X-ray diffraction were grown by a slow vapor diffusion of diethyl ether into a methanol solution containing the zinc complex. Anal. Calc. for C<sub>42</sub>H<sub>58</sub>Cl<sub>6</sub>N<sub>10</sub>S<sub>4</sub>Zn<sub>3</sub> • 2 H<sub>2</sub>O (1240.09): C, 39.53; H, 4.90; N, 10.98. Found: C, 39.60, H, 4.80, N, 10.85.

$^1\text{H}$  NMR (DMSO- $d_6$ , 300 MHz)  $\delta$  7.72 (m, 1H, pyridine CH), 7.22 (d ( $^3J = 2.4$  Hz), 2H, imidazole CH), 7.19 (d ( $^3J = 2.4$  Hz), 2H, imidazole CH) 6.89 (d ( $^3J = 7.8$  Hz), 2H, pyridine CH), 5.28 (s, 4H,  $\text{CH}_2$ ), 3.97 (t ( $^3J = 7.5$  Hz), 4H, *n*-butyl  $\text{CH}_2$ ), 1.68 (m, 4H, *n*-butyl  $\text{CH}_2$ ), 1.29 (m, 4H, *n*-butyl  $\text{CH}_2$ ), 0.903 (t ( $^3J = 7.2$ Hz), 6H, *n*-butyl  $\text{CH}_3$ ).

$^{13}\text{C}\{^1\text{H}\}$  NMR (DMSO- $d_6$ , 75 MHz),  $\delta$  161.79 (C=S), 155.82 (pyridine  $\text{C}_{\text{ipso}}$ ), 137.77 (pyridine CH), 119.96 (pyridine CH), 117.95 (imidazole CH), 117.65 (imidazole CH), 51.35 ( $\text{CH}_2$ ), 46.65 (*n*-butyl  $\text{CH}_2$ ), 30.37 (*n*-butyl  $\text{CH}_2$ ), 19.11 (*n*-butyl  $\text{CH}_2$ ), 13.55 (*n*-butyl  $\text{CH}_3$ ).

$^1\text{H}$  NMR (MeOH- $d_4$  300 MHz)  $\delta$  7.90 (m, 1H, pyridine CH), 7.47 (d ( $^3J = 7.8$  Hz), 2H, pyridine CH), 7.28 (AB doublet ( $^3J = 2.1$  Hz), 2H, imidazole CH) 7.23 (AB doublet ( $^3J = 2.4$  Hz), 2H, imidazole CH), 5.54 (s, 4H,  $\text{CH}_2$ ), 4.11 (t ( $^3J = 7.5$  Hz), 4H, *n*-butyl  $\text{CH}_2$ ), 1.79 (m, 4H, *n*-butyl  $\text{CH}_2$ ), 1.38 (m, 4H, *n*-butyl  $\text{CH}_2$ ), 0.98 (t ( $^3J = 7.5$ Hz), 6H, *n*-butyl  $\text{CH}_3$ ).

**2.5.15 Synthesis of chloro-( $\eta^3$ -S,S,N)-[2,6-bis(N-isopropyl-N'-methylenetriazole-2-thione)pyridine]zinc(II) aquatrichlorozincate  $[\text{C}_{17}\text{H}_{23}\text{N}_7\text{S}_2\text{ZnCl}][\text{ZnCl}_3(\text{H}_2\text{O})]$  [4]**

Yield: 0.24 g (quantitative). The white product was precipitated by a slow vapor diffusion of diethyl ether into an acetonitrile solution containing the zinc complex. Anal. Calc. for  $\text{C}_{17}\text{H}_{25}\text{Cl}_4\text{N}_7\text{OS}_2\text{Zn}_2 \cdot 1 \text{H}_2\text{O}$  (680.13): C, 29.25; H, 3.90; N, 14.04. Found: C, 29.04 H, 3.64, N, 13.59.

$^1\text{H}$  NMR (DMSO- $d_6$ , 300 MHz)  $\delta$  8.44 (s, 2H, triazole CH), 7.81 (m, 1H, pyridine CH), 7.25 (d ( $^3J = 7.8$  Hz), 2H, pyridine CH), 5.27 (s, 4H,  $\text{CH}_2$ ), 4.91 (m, 2H, isopropyl CH), 1.33 (d ( $^3J = 6.6$  Hz), 12H, isopropyl  $\text{CH}_3$ ).  $^{13}\text{C}\{^1\text{H}\}$  NMR (DMSO- $d_6$ , 75 MHz),  $\delta$

164.02 (C=S), 154.11 (pyridine C<sub>ipso</sub>), 141.34 (triazole CH), 137.96 (pyridine CH), 121.11 (pyridine CH), 49.77 (isopropyl CH), 48.85 (CH<sub>2</sub>), 20.50 (isopropyl CH<sub>3</sub>).

<sup>1</sup>H NMR (MeOH-d<sub>4</sub>, 300 MHz) δ 8.24 (s, 2H, triazole CH), 7.78 (t (<sup>3</sup>J = 7.5 Hz), 1H, pyridine CH), 7.34 (d (<sup>3</sup>J = 7.5 Hz), 2H, pyridine CH), 5.32 (s, 4H, CH<sub>2</sub>), 5.05 (m, 2H, isopropyl CH), 1.38 (d (<sup>3</sup>J = 4.8 Hz), 12H, isopropyl CH<sub>3</sub>). <sup>13</sup>C {<sup>1</sup>H} NMR (MeOH-d<sub>4</sub>, 75 MHz) δ 165.55 (C=S), 155.48 (C<sub>ipso</sub>), 142.29 (CH triazole), 139.15 (CH pyridine), 122.98 (CH pyridine), 51.88 (CH isopropyl), 50.47 (CH<sub>2</sub>), 20.99 (CH<sub>3</sub> isopropyl)

**2.5.16 Synthesis of chloro-(η<sup>3</sup>-S,S,N)-[2,6-bis(N-neopentyl-N'-methylenetriazole-2-thione)pyridine]zinc(II) trichlorozincate ([C<sub>21</sub>H<sub>31</sub>N<sub>7</sub>S<sub>2</sub>ZnCl][ZnCl<sub>3</sub>]), [5]:**

Yield: 0.25g (quantitative). The product was purified by precipitation by dissolving the product in methanol and allowing for a slow vapor diffusion of diethyl ether into the methanol solution. Anal. Calc. for C<sub>21</sub>H<sub>31</sub>Cl<sub>4</sub>N<sub>7</sub>OS<sub>2</sub>Zn<sub>2</sub> • CH<sub>3</sub>OH (718.22): C, 35.22; H, 4.70; N, 13.07. Found: C, 35.90 H, 5.20, N, 13.73.

<sup>1</sup>H NMR (DMSO-d<sub>6</sub>, 300 MHz) δ 8.49 (s, 1H, triazole CH), 7.81 (m, 1H, pyridine CH), 7.19 (d (<sup>3</sup>J = 7.8 Hz), 2H, pyridine CH), 5.28 (s, 4H, CH<sub>2</sub>), 3.98 (s, 4H, neopentyl CH<sub>2</sub>), 0.97 (s, 18H, neopentyl CH<sub>3</sub>). <sup>13</sup>C {<sup>1</sup>H} NMR (DMSO-d<sub>6</sub>, 75 MHz), δ 166.75 (C=S), 154.18 (pyridine C<sub>ipso</sub>), 141.10 (triazole CH), 137.95 (pyridine CH), 120.80 (pyridine CH), 58.33 (neopentyl CH<sub>2</sub>), 49.31 (CH<sub>2</sub>), 33.61 (C(CH<sub>3</sub>)<sub>3</sub>), 27.75 (CH<sub>3</sub>).

<sup>1</sup>H NMR (MeOH-d<sub>4</sub>, 300 MHz) δ 8.24 (s, 1H, triazole CH), 7.78 (t (<sup>3</sup>J = 7.5 Hz), 1H, pyridine CH), 7.32 (d (<sup>3</sup>J = 7.8 Hz), 2H, pyridine CH), 5.33 (s, 4H, CH<sub>2</sub>), 4.05 (s, 4H, neopentyl CH<sub>2</sub>), 1.02 (s, 18H, neopentyl CH<sub>3</sub>). <sup>13</sup>C {<sup>1</sup>H} NMR (MeOH-d<sub>4</sub>, 75 MHz), δ 168.46 (C=S), 155.51 (pyridine C<sub>ipso</sub>), 141.93 (triazole CH), 139.12 (pyridine CH),

122.77 (pyridine CH), 60.27 (neopentyl CH<sub>2</sub>), 50.89 (CH<sub>2</sub>), 34.90 (C(CH<sub>3</sub>)<sub>3</sub>), 28.44 (CH<sub>3</sub>).

**2.5.17 Synthesis of chloro-( $\eta^3$ -S,S,N)-{2,6-bis[(N-(*n*-butyl)-N'-methylenetriazole-2-thione]pyridine}zinc(II) bis( $\mu$ -chlorodichlorozincate) ([C<sub>38</sub>H<sub>54</sub>N<sub>14</sub>S<sub>4</sub>Zn<sub>2</sub>Cl<sub>2</sub>][Zn<sub>2</sub>Cl<sub>6</sub>]  
[6]**

Yield: 0.28 g (quantitative). Crystals suitable for X-ray diffraction analysis were grown by allowing diethyl ether vapor to slowly diffuse into a solution of **6** in methanol.

Anal. Calc. for C<sub>19</sub>H<sub>29</sub>Cl<sub>4</sub>N<sub>7</sub>OS<sub>2</sub>Zn<sub>2</sub> • H<sub>2</sub>O • CH<sub>3</sub>OH (708.18): C, 31.68; H, 4.65; N, 12.93. Found: C, 31.51, H, 4.06, N, 12.57.

<sup>1</sup>H NMR (DMSO-d<sub>6</sub>, 300 MHz)  $\delta$  8.45 (s, 2H, triazole CH), 7.81 (m, 1H, pyridine CH), 7.23 (d (<sup>3</sup>J = 7.8 Hz), 2H, pyridine CH), 5.26 (s, 4H, CH<sub>2</sub>), 4.09 (t (<sup>3</sup>J = 6.9 Hz), 4H, *n*-butyl CH<sub>2</sub>), 1.73 (m, 4H, *n*-butyl CH<sub>2</sub>), 1.28 (m, 4H, *n*-butyl CH<sub>2</sub>), 0.90 (t (<sup>3</sup>J = 7.2 Hz), 6H, *n*-butyl CH<sub>3</sub>). <sup>13</sup>C {<sup>1</sup>H} NMR (DMSO-d<sub>6</sub>, 75 MHz),  $\delta$  165.11 (C=S), 154.09 (pyridine C<sub>ipso</sub>), 141.36 (pyridine CH), 137.95 (triazole CH), 120.95 (pyridine CH), 49.06 (CH<sub>2</sub>), 48.00 (*n*-butyl CH<sub>2</sub>), 29.57 (*n*-butyl CH<sub>2</sub>), 19.05 (*n*-butyl CH<sub>2</sub>), 13.45 (*n*-butyl CH<sub>3</sub>).

<sup>1</sup>H NMR (MeOH-d<sub>4</sub>, 300 MHz)  $\delta$  8.22 (s, 2H, triazole CH), 7.78 (m, 1H, pyridine CH), 7.33 (d (<sup>3</sup>J = 7.8 Hz), 2H, pyridine CH), 5.31 (s, 4H, CH<sub>2</sub>), 4.18 (t (<sup>3</sup>J = 7.2 Hz), 4H, *n*-butyl CH<sub>2</sub>), 1.82 (m, 4H, *n*-butyl CH<sub>2</sub>), 1.36 (m, 4H, *n*-butyl CH<sub>2</sub>), 0.97 (t (<sup>3</sup>J = 7.5 Hz), 6H, *n*-butyl CH<sub>3</sub>). <sup>13</sup>C {<sup>1</sup>H} NMR (MeOH-d<sub>4</sub> 75 MHz),  $\delta$  166.68 (C=S), 155.40 (pyridine C<sub>ipso</sub>), 142.29 (pyridine CH), 139.13 (triazole CH), 122.79 (pyridine CH), 50.62 (CH<sub>2</sub>), 49.96 (*n*-butyl CH<sub>2</sub>), 31.16 (*n*-butyl CH<sub>2</sub>), 20.68 (*n*-butyl CH<sub>2</sub>), 13.97 (*n*-butyl CH<sub>3</sub>).

### 3. Results and Discussion:

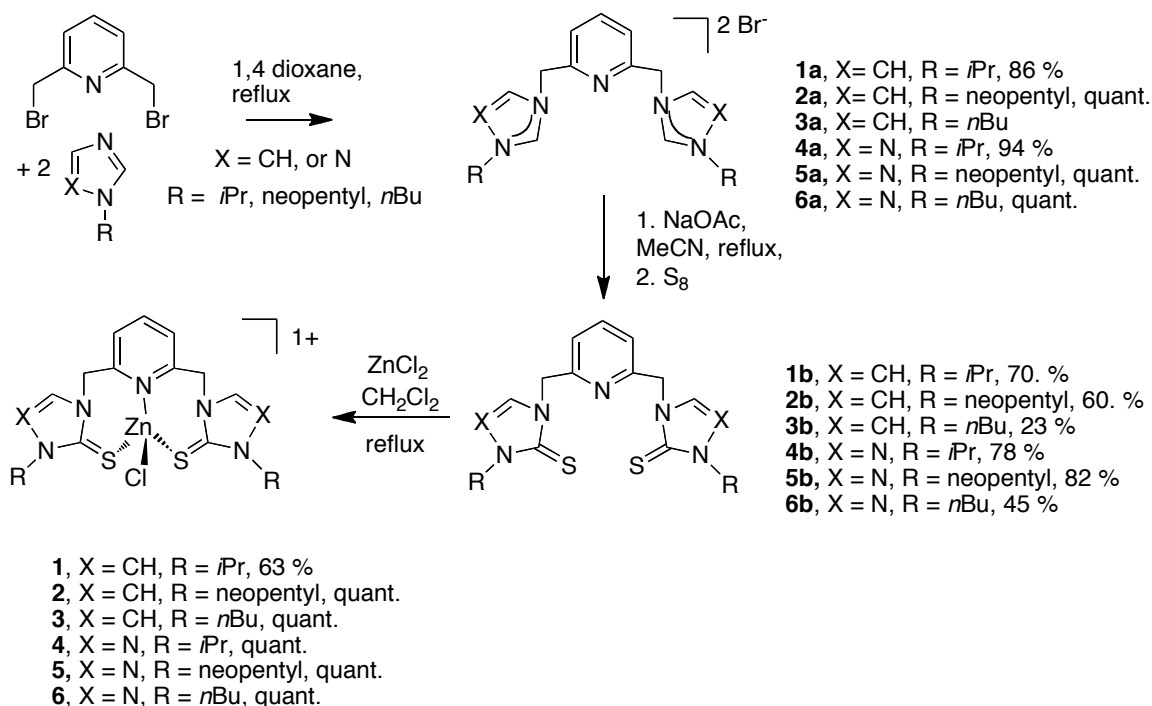
#### 3.1 Syntheses and Spectroscopy

The syntheses of the tridentate SNS ligand precursors and zinc complexes **1 - 6** were accomplished following Scheme 1. Different R groups were employed because Crabtree has reported that modification of such substituents affects the solubility and catalytic activity of the metal complexes [25]. The alkyl imidazoles or alkyl triazoles were prepared either by following known routes or were commercially available [24-27]. These compounds react with 2,6-bis(bromomethyl)pyridine in 1,4-dioxane to form ligand precursor salts, **1a - 6a**, that are soluble in DMSO, methanol, acetonitrile and water [20, 28].

Compounds **1a - 6a** react with a mild base, sodium acetate, and elemental sulfur in refluxing acetonitrile to form bis-thione ligand precursors **1b - 6b** [24]. As determined by NMR spectroscopy, compounds **1b - 6b** can be purified by filtering a dichloromethane solution containing this compound through alumina. The bis-thione ligand precursors are soluble in DMSO, dichloromethane, chloroform, acetone, acetonitrile, and methanol. Off-white crystals of **5b** that were suitable for X-ray diffraction were grown by allowing diethyl ether to slowly diffuse into a solution of **5b** in acetonitrile.

The bis-thione ligand precursors subsequently react with ZnCl<sub>2</sub> in refluxing CH<sub>2</sub>Cl<sub>2</sub> to afford zinc complexes **1 - 6**. The driving force for the metallation is the formation of zinc complexes **1-6**, which are sparingly soluble in CH<sub>2</sub>Cl<sub>2</sub>. Off-white crystals that were suitable for X-ray diffraction were grown by allowing diethyl ether vapor (**1, 3, and 6**) to slowly diffuse into an acetonitrile (**1**) or methanol (**3** or **6**) solution containing the zinc complex. All of the reactions could be carried out in air, and proceeded in yields at or

above 63 %. The zinc complexes **1-6** are soluble in DMSO, acetonitrile, methanol, and water and are sparingly soluble in dichloromethane and chloroform. Complexes **4-6** were more soluble in MeOH- $d_4$  than were **1-3**.



**Scheme 1:** Preparation of **1-6**

Ligand precursors **1a – 6a** and **1b – 6b** and zinc complexes **1-6** were characterized using  $^1\text{H}$ ,  $^{13}\text{C}$ , and HSQC NMR spectroscopy. For all compounds, only one set of resonances was detected indicating that the two halves of each molecule are symmetry-related. The  $^{13}\text{C}$  NMR of **1b - 3b** and of **4b - 6b**, show resonances at  $\delta \sim 162$  ppm and  $\delta \sim 166$  ppm, respectively, that are consistent with C=S formation [17]. The ligand precursors **1a – 6a** contain a resonance at  $\delta \sim 11$  ppm in their  $^1\text{H}$  NMR spectra indicative of an acidic C-H proton whereas this feature is absent in the spectra of compounds **1b – 6b** in which the proton has been replaced by a sulfur atom.

Attenuated total reflectance IR spectra were collected for **1b** – **6b**. The C=S stretch occurs at 1128 to 1129  $\text{cm}^{-1}$  for the bis-imidazole bis-thione precursors (**1b-3b**) and at 1144 to 1158  $\text{cm}^{-1}$  for the bis-triazole bis-thione systems, **4b** – **6b**. This data is consistent with the triazole compounds having stronger C=S bonds.

Complexes **1-6** were analyzed with  $^1\text{H}$ ,  $^{13}\text{C}$ , and HSQC NMR spectroscopy in DMSO- $\text{d}_6$ . The  $^1\text{H}$  and  $^{13}\text{C}$  NMR of the zinc complexes are identical to the respective ligand precursors **1b** – **6b**, with very little shift in the resonances. This was expected since no hydrogen or carbon atoms are displaced or added upon metallation with zinc(II) chloride. In addition, the  $^1\text{H}$  NMR spectra of complexes **1-6** were acquired in a less polar and weakly coordinating solvent, MeOH- $\text{d}_4$ , to verify that the SNS pincer ligands are not displaced from the coordination sphere of zinc. Electrospray mass spectrometry data, described below, also verifies this result. Zinc complexes **4-6** are more soluble than zinc complexes **1-3** in MeOH- $\text{d}_4$ . We were able to prepare NMR samples of complexes **4-6** that were concentrated enough in MeOH- $\text{d}_4$  so that we could acquire a  $^{13}\text{C}$  NMR spectrum of these complexes. In the  $^1\text{H}$  NMR spectra that were acquired in MeOH- $\text{d}_4$  for complexes **1-3**, when compared to the  $^1\text{H}$  NMR spectra acquired in DMSO- $\text{d}_6$ , the resonances generally shifted at least  $\delta$  0.10 ppm upfield. For complexes **1-3**, the pyridine CH doublet shifted at least  $\delta$  0.55 ppm upfield in the proton NMR spectra that were acquired in MeOH- $\text{d}_4$ , when compared to the  $^1\text{H}$  NMR spectra acquired in DMSO- $\text{d}_6$ . In the  $^1\text{H}$  NMR spectra that were acquired in MeOH- $\text{d}_4$  for complexes **4-6**, when compared to the  $^1\text{H}$  NMR spectra acquired in DMSO- $\text{d}_6$ , some of the resonances shifted upfield and others shifted downfield. The  $^{13}\text{C}$  NMR resonances for complexes **4-6**

shifted at least  $\delta$  0.4 ppm upfield in MeOH- $d_4$  when compared to the spectra obtained in DMSO- $d_6$ .

ESI-MS spectra for compounds **1-6** were collected with cone voltages of 0 V and 70 V. The predominant feature in the spectra of these systems at the higher cone voltage is that of the fully ligated zinc complex, indicating that the compound is stable and suggesting that it is unlikely that the ligand is displaced when dissolved in a polar solvent. In negative ion mode, the expected  $m/z$  values were seen for  $[\text{ZnCl}_3]^-$ . The isotopic patterns in the mass spectrometry data fit the assigned structures.

### 3.2 X-ray Crystallography

The solid-state molecular structures of **1**, **3**, **5b**, and **6** are shown in Figures 2-5, respectively. Analogous to the LADH structure, complexes **1**, **3**, and **6** feature a zinc atom that is tetrahedrally coordinated. These complexes also feature SNS donor atoms and pseudotetrahedral geometry about the zinc center, as is seen for liver alcohol dehydrogenase. The bond lengths and bond angles compare reasonably well to the active site of horse LADH enzyme bound to NADH (Table 2) [33].

The carbon-sulfur bond lengths for **1**, **3**, and **6** were between 1.65 – 1.70 Å (Table 2). These bond lengths are between what is normally associated with a C-S single bond, 1.83 Å, and a C=S double bond, 1.61 Å [34]. For **1** and **3**, the counter-anion is  $[\text{ZnCl}_4]^{2-}$  and for **6**, the counter ion is  $[\text{Zn}_2\text{Cl}_6]^{2-}$ . The counter-ion is seen even when either one or two molar equivalents of  $\text{ZnCl}_2$  are used in the preparation of **1-6**. In complex **1**, two molecules of acetonitrile co-crystallized within the unit cell. The R-factor for **3** was 0.09 and was higher than the R-factor reported for **1**, **5b**, or **6** (Table 1). The higher R-factor

for **3** could be attributed to disorder in the *n*-butyl groups present in the zinc complex [21].

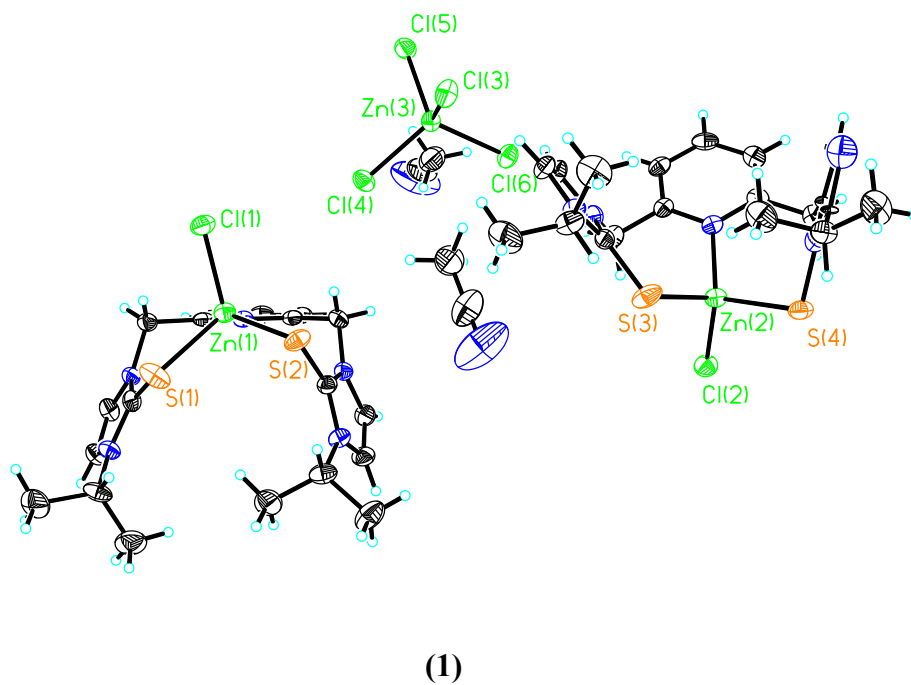
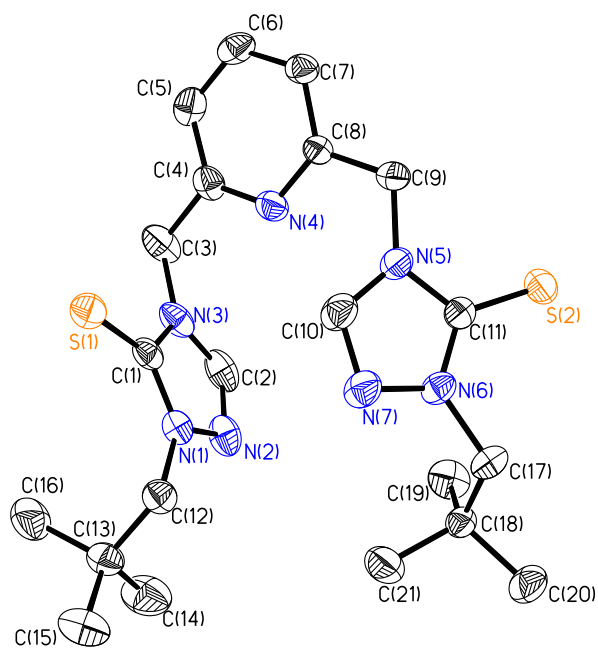


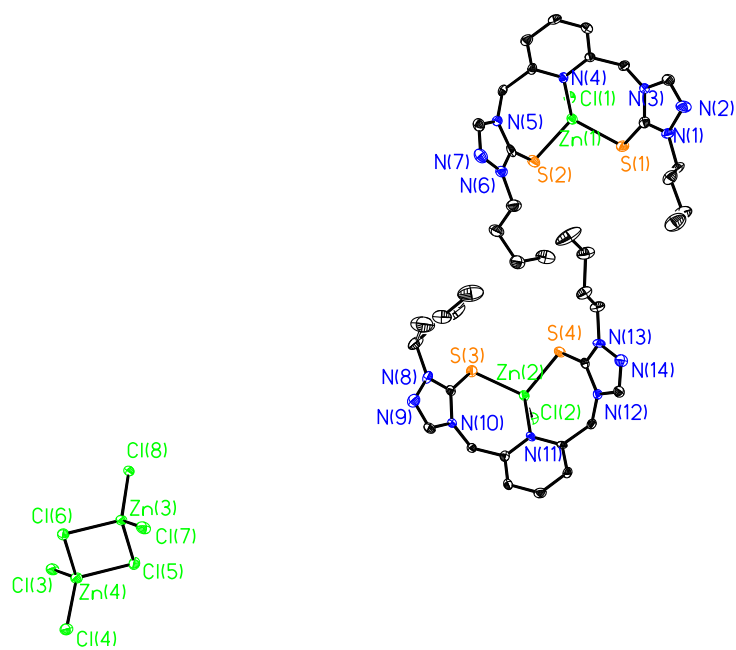
**Figure 2.** Solid-state structure of complex **1**.





(5b)

Figure 4. Solid-state structure of complex 5b.



(6)

**Figure 5.** Solid-state structure of complex 6.

**Table 2.** Selected bond lengths and angles (esd) for **1**, **3**, and **6** with comparison to LADH-NADH [33].

	R = iPr ( <b>1</b> )	R = nBu ( <b>3</b> )	R = nBu ( <b>6</b> )	LADH-NADH
Zn(1) – N(1)	2.107(3)	1.972(11)	2.057(4)	2.15
(Å)				
Zn(1) – Cl(1)	2.2249(13)	2.219(5)	2.2500(12)	
(Å)				
Zn(1) – S(1)	2.3387(14)	2.321(4)	2.3541(14)	2.32
(Å)				
Zn(1) – S(2)	2.3510(14)	2.321(4)	2.3277(14)	2.23
(Å)				
S(1) – C(1) (Å)	1.700(4)	1.650(12)	1.702(5)	
N(3) – Zn(1) – Cl(1)	107.50(10)	99.0(4)	100.39(10)	
N(3) – Zn(1) – S(1)	109.76(10)	125.0(5)	115.04(11)	105
Cl(1) – Zn(1) – S(1)	114.24(5)	118.6(2)	111.22(5)	
N(3) – Zn(1) – S(2)	114.37(10)	100.3(4)	115.71(11)	114
Cl(1) – Zn(1) – S(2)	109.55(4)	115.25(16)	113.36(5)	

---

S(1) – Zn(1) –	101.54(5)	99.16(15)	101.62(5)	130
S(2)				

---

Various parameters of the Gaussian 03-optimized structures for the ligands compare favorably with the crystal structure determined for compound **5b** (Figure 4). In particular, the calculated C=S bond lengths of 1.675 Å (X=N and R = CH<sub>3</sub>) and 1.683 Å (X = CH and R = CH<sub>3</sub>) are quite close to those found for **5b** (1.677 Å and 1.667 Å). Similarly, the N-N bond length calculated for the triazole ligand (1.375 Å) matches that determined for **5b** (1.385 Å) as do the C-NN (1.362 Å vs. 1.353 Å, respectively) and the C-NCH<sub>2</sub> (1.390 Å vs. 1.373 Å, respectively) bond lengths. The use of B3LYP/6-31G\* method to model the electrochemical behavior of this ligand as discussed in the following section of this report is therefore justified.

### ***3.3 Cyclic Voltammetry of Ligand Precursors and Comparison of Cyclic Voltammetry Results to Gaussian Calculations.***

Compounds **1b** and **5b** were studied by cyclic voltammetry in DMSO as part of their characterizations. The cyclic voltammogram for **1b** (Figure 6) shows oxidation waves at 976 and 1339 mV (the latter caused most likely by solvent degradation) while the cyclic voltammogram for **5b** (Figure 7) has a wave at 1178 mV. The oxidation waves are broad and are located at the same potential across consecutive scans, indicating the stability of the ligands with respect to repeated oxidation and reduction. To understand the nature of this electrochemical feature, we chose to perform quantum mechanical calculations using Gaussian 03.

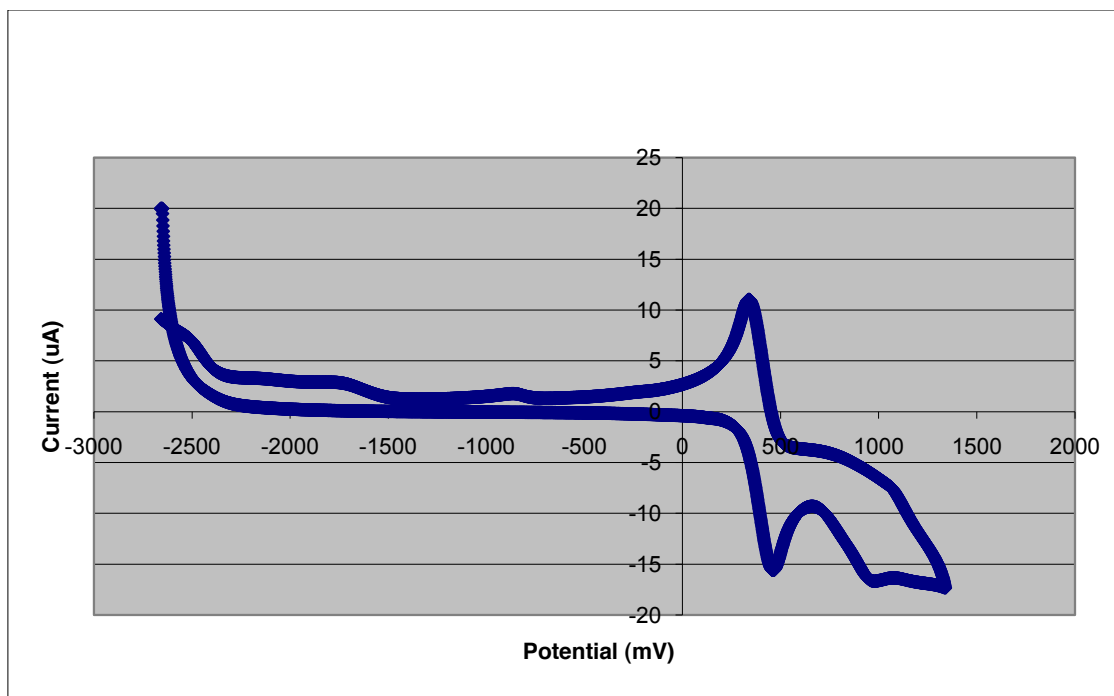


**Figure 6.** Cyclic Voltammogram of **1b** in DMSO (2mM) with 0.2 M TBAF. The scan rate was 100 mV/s with ferrocene ( $E_{1/2} = 400$  mV) used as an internal standard.

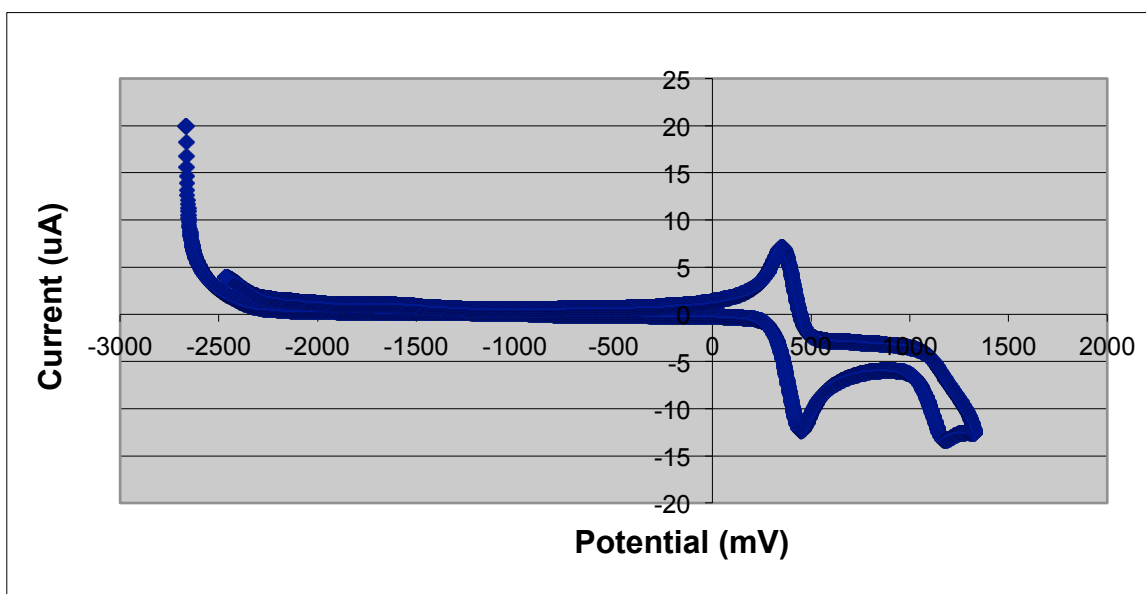


**Figure 7.** Cyclic Voltammogram of **5b** in DMSO (2mM) with 0.2 M TBAF. The scan rate was 100 mV/s with ferrocene ( $E_{1/2} = 400$  mV) used as an internal standard.

The Gaussian calculations performed as part of this study agree quite well with the experimentally observed oxidation potentials for the pincer ligand and shed light on how the degree of through-space interaction of the thioimidazole/thiotriazole rings can impact the observed oxidation potential. The  $\Delta G$  oxidation potentials for the solvated bis-thioimidazole system are calculated to be 0.828 V with the ligand structure constrained to  $C_s$  symmetry and 1.234 V under  $C_2$  symmetry. For the bis-thiotriazole compound, the calculated oxidation potentials are 1.178 V ( $C_s$ ) and 1.716 V ( $C_2$ ). For both ligands, the oxidation potential determined under  $C_s$  symmetry correlates well with the experimentally determined value, with that calculated for the triazole system matching the experimental value exactly. Also of note is the relative oxidation potentials, both calculated and experimentally determined, between the thioimidazole and thiotriazole systems. Replacement of a C-H unit in the imidazolyl ring with a more electronegative N atom causes the oxidation to become more difficult by ca. 200 mV.

The imposition of  $C_s$  symmetry on the ligand forces the thione-containing rings to stack while under the  $C_2$  point group, the thioimidazole/thiotriazole rings are located on opposite sides of the connecting pyridine ring. For reference, the optimized structures of the neutral  $C_s$ - and  $C_2$ -symmetry structures are presented in Figure 8. Of particular note is the sulfur-sulfur distance between the two rings, which for the neutral optimized structures is 6.97Å for the  $C_s$  structure and 10.22Å for the  $C_2$  system. For the cations, the S-S distance under the  $C_s$  point group decreases considerably to 3.03Å while it remains

largely the same (10.15Å) for the  $C_2$  structure. Examination of a contour plot of the HOMO for the bis-thioimidazole system, shown in Figure 9, explains this observation. This orbital contains S, N, and C  $\pi$  character and is located entirely on the thioimidazole rings, with a considerable amount of the orbital character residing on the S atoms in a  $\sigma^*$  fashion between the sulfurs. Removal of an electron from this orbital acts to decrease the S-S repulsive nature of this orbital, which explains the more than halving of the S-S distance observed in the geometry optimizations upon oxidation of this system. Similar systems are known to form disulfides upon oxidation [35], which leads us to conclude that inclusion of a strong S-S interaction through the imposition of the  $C_s$  point group is essential for an acceptable computational modeling of the oxidation potential. We also note that this interaction, permitted by the flexibility allowed through the introduction of the methylene linkers, leads to an oxidation that is approximately 300 mV easier than we observed in our previous report. [20]

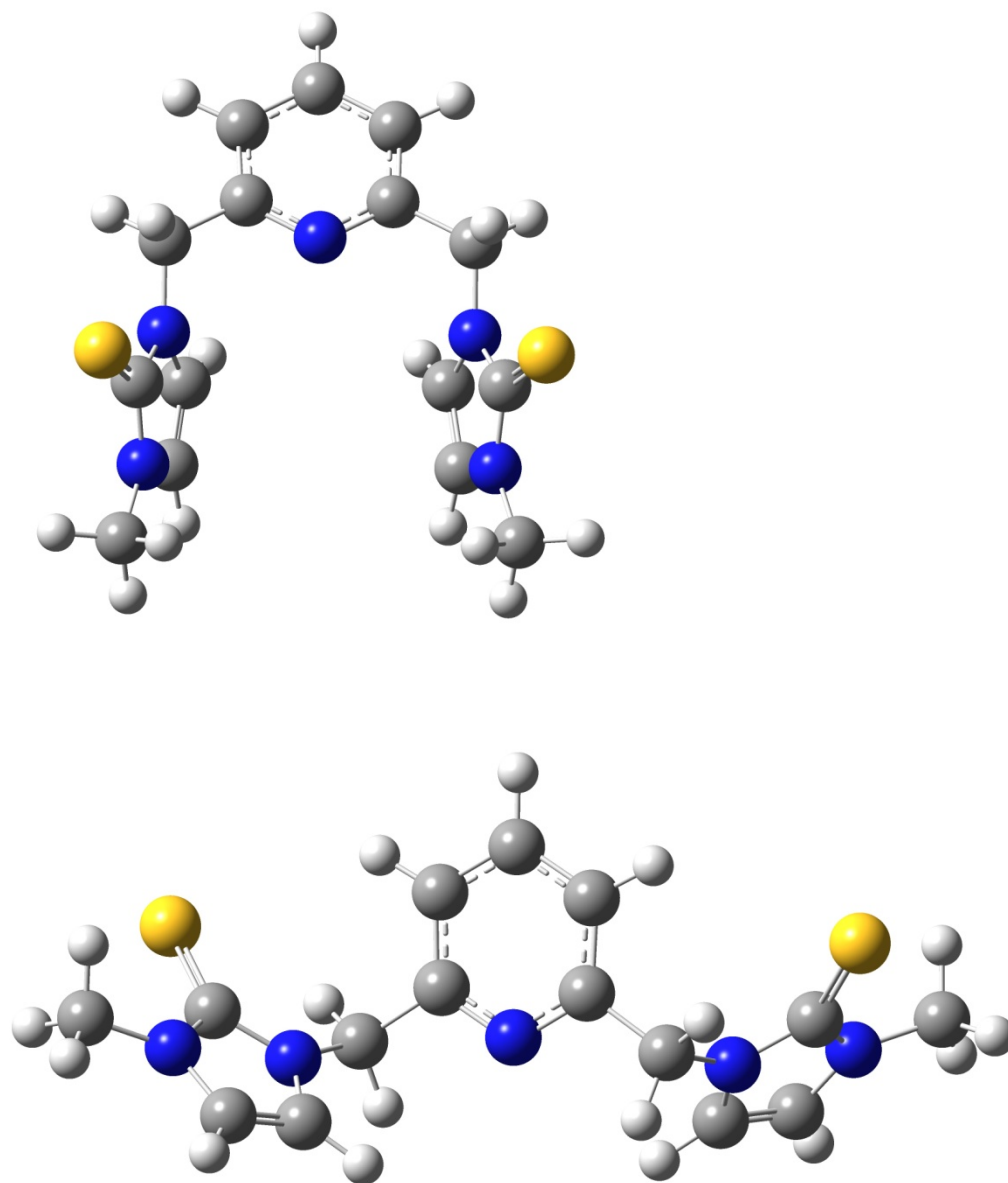


**Figure 8.** Optimized structures of thioimidazole systems having  $C_s$  (top) and  $C_2$  (bottom) symmetry. Hydrogen atoms are white, carbons are grey, nitrogens are blue, and sulfurs are yellow.

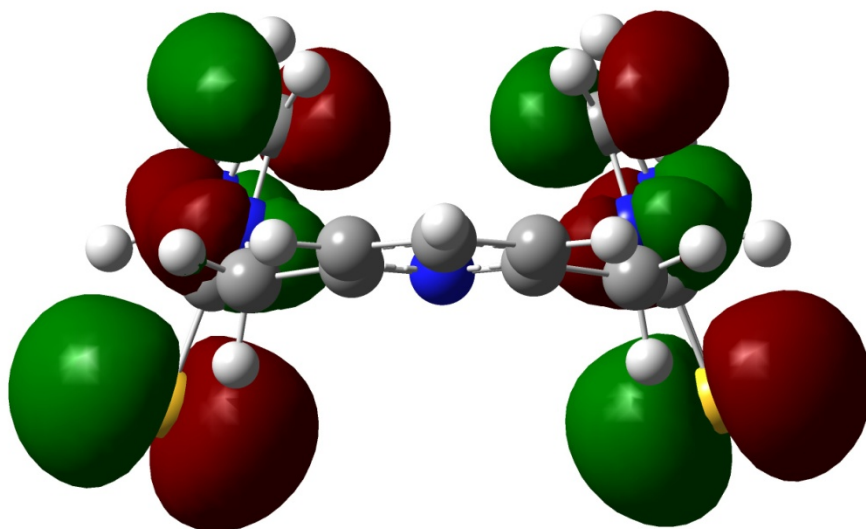


**Figure 9.** Contour plot of bis-thioimidazole ligand HOMO as viewed from above the pyridinyl ring. This orbital contains  $\pi$ -type character on the thioimidazole rings with a  $\sigma^*$ -like interaction between the p orbitals on the S atoms as seen in the bottom portion of this contour plot.

### 3.5 Reactivity

With an established synthetic protocol for these metalloenzyme models and a greater understanding of their structural characteristics, our attention was turned to probing their stoichiometric activity. Zinc complexes **1-6** were screened for activity through the reduction of 4-nitrobenzaldehyde, an electron-poor aldehyde, in the presence of a hydrogen donor, 1-benzyl-1,4-dihydronicotinamide (BNAH) (eq. 1). BNAH was prepared following a known literature procedure and is the reagent of choice to model NADH [28].  $^1\text{H}$  NMR was used to follow the disappearance of the aldehyde proton ( $\delta$  10.2 ppm) and the shifting of the aromatic C-H protons in the alcohol product ( $\delta$  8.24

ppm). The aromatic proton resonances of the C-H protons in the alcohol product were spectroscopically distinct from the other product or starting materials resonances and no overlap of  $^1\text{H}$  NMR resonances was observed. For all reactivity experimentation, 0.1 mmol of aldehyde, 0.1 mmol zinc precursor or 0.2 mmol of  $\text{ZnCl}_2$ , and 0.2 mmol BNAH were used. Control reactions with  $\text{ZnCl}_2$  were performed using two equivalents of this salt because complexes **1-6** contain two zinc ions (one in the cation and one in the anion) per neutral compound. Product formation was detected by  $^1\text{H}$  NMR by comparison with authentic material. In no case was there any indication of reduction of nitro substituents. Table 3 illustrates the reactivity data for **1-6** as well as for  $\text{ZnCl}_2$  and the ligand precursor.

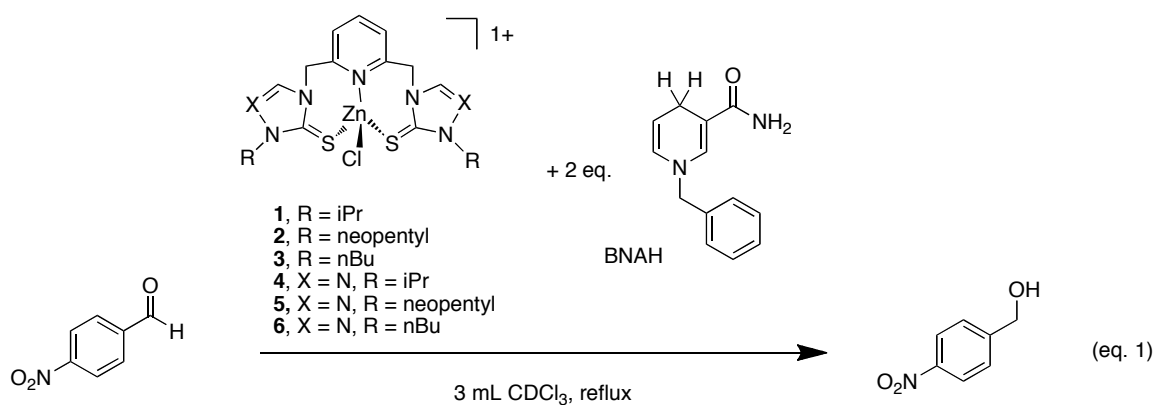


**Table 3.** Reactivity Data for **1-6**

Entry	Zn Complex	Time	Conversion (%)
1	None	20h	< 5
2	<b>2b</b> (bis thione ligand precursor)	20h	< 5
3	ZnCl <sub>2</sub> (2 eq.)	5h	15
4	ZnCl <sub>2</sub> <sup>a</sup> (2 eq.)	20h	13
5	ZnCl <sub>2</sub> (2 eq.)	20h	18
6	<b>1</b>	20h	32
7	<b>2</b>	20h	23
8	<b>3</b>	20h	25
9	<b>4</b>	20h	37
10	<b>5</b>	20h	45
11	<b>6</b>	20h	59
12	ZnCl <sub>2</sub> (10 eq.)	20h	42

<sup>a</sup> Reaction was run under an N<sub>2</sub> environment. The reaction was setup in an inert atmosphere glove box.

As shown in Table 3, zinc complexes **1-6** enhance the rate of the reaction for the reduction of 4-nitrobenzaldehyde when compared to that for either ZnCl<sub>2</sub> or ligand precursor. Mechanistically, others have proposed a hydrogen atom transfer between the co-factor and the substrate upon coordination to the zinc active site based upon a previously reported mechanism for LADH offered by Berreau and co-workers [36]. Entries 3-5 in Table 3 indicate that ZnCl<sub>2</sub> reacts stoichiometrically with electron-poor aldehydes such as 4-nitrobenzaldehyde to yield alcohol product to a small extent (ca. 18 % conversion). We therefore propose that Zn<sup>2+</sup> acts as a Lewis acid catalyst in the reaction where ZnCl<sub>2</sub> is utilized. It is plausible that the Zn<sup>2+</sup> in the counteranion contributes to the reactivity that is shown for **1-6** in Table 3. Experiments are underway to prepare tridentate zinc SNS pincer complexes with a counter-anion that does not contain a zinc ion. We also wondered if an excess of ZnCl<sub>2</sub> would enhance the rate of conversion of 4-nitrobenzaldehyde. We saw 42 % conversion of 4-nitrobenzaldehyde after 20 h when

excess  $\text{ZnCl}_2$  (10 eq) was used. Thus, an excess of  $\text{ZnCl}_2$  and BNAH could also be used to reduce 4-nitrobenzaldehyde.

Reactivity data for imidazole complexes with the  $\text{CH}_2$  linker is consistently lower when compared to previous studies carried out without the  $\text{CH}_2$  linker [20] when identical ligand groups were tested. Imidazole compounds with isopropyl wingtip R groups without the  $\text{CH}_2$  linker gave a catalytic activity of 42% compared to 32% when the  $\text{CH}_2$  linker compound was tested. Similarly, the zinc complexes with neopentyl wingtip groups and no  $\text{CH}_2$  linker had a greater turnover (48 %) than did the analogous compound with a methylene linker (23 %), and the zinc complexes with *n*-butyl wingtip groups and no  $\text{CH}_2$  linker had a greater turnover (33 %) and the identical compounds with a  $\text{CH}_2$  linker (25 %).

Based on the data presented in Table 3, it appears that the choice of the alkyl group is important as *n*-butyl and neopentyl groups (bis-triazole) gave a higher percent conversion than isopropyl. Previous experimentation without the  $\text{CH}_2$  linker supported the claim that isopropyl wingtips yielded the greatest catalytic activity due to the fact that larger R groups such as *n*-butyl are more sterically demanding, when compared to neopentyl or isopropyl, and may shield the zinc metal center from interacting with BNAH and substrate. The opposite trend was observed for both imidazole and triazole complexes with the  $\text{CH}_2$  linker. Perhaps added room for binding provided by the  $\text{CH}_2$  linker reduces the wingtip effects previously observed. Furthermore, the larger R group complexes gave the greatest solubility. The identity of the wingtip group is therefore a crucial variable to consider when screening metal complexes for activity [22].

The choice of azole rings also is important as CH<sub>2</sub> linker complexes with the triazole ring gave consistently greater catalytic activity for the reduction reaction than identical R group imidazole complexes. The system with the greatest catalytic efficiency was complex **6** (59 %), which contains triazole rings that possess *n*-butyl wingtip groups.

We also tried to reduce another electron-poor aldehyde, pyridine-2-carboxaldehyde, in the presence of a stoichiometric amount of **1-6** or ZnCl<sub>2</sub> (eq. 2). <sup>1</sup>H NMR was used to follow the disappearance of the aldehyde proton (δ 10.2 ppm) and the appearance of the aromatic C-H protons in the alcohol product (δ 8.4 ppm). The aromatic proton resonance of the alcohol product did not overlap with the <sup>1</sup>H NMR resonances of either the starting materials or the products or the zinc complex. Table 4 illustrates the reactivity data for **1-6** as well as for ZnCl<sub>2</sub>.

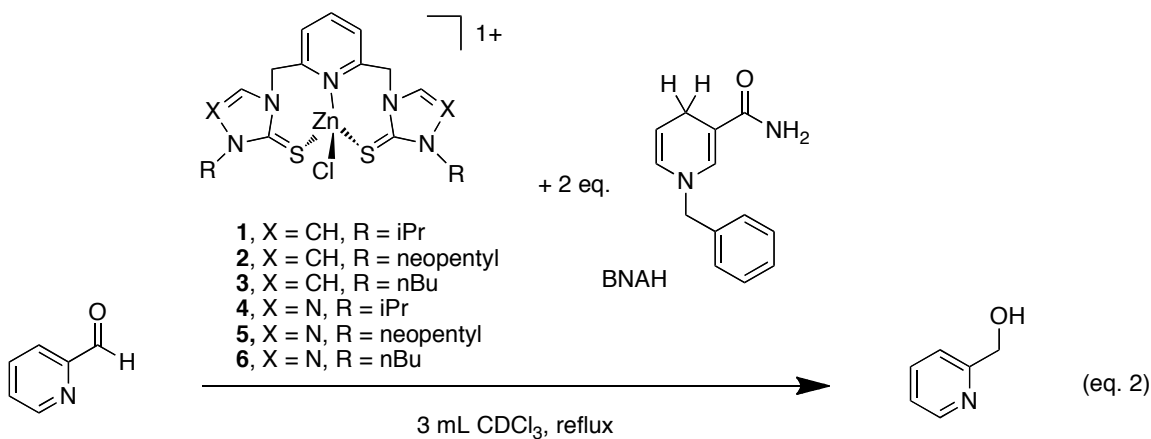


**Table 4.** Reactivity Data for **1-6** for the reduction of pyridine-2-carboxaldehyde.

Entry	Zn Complex	Time	Conversion (%)
1	None	20h	< 5
2	ZnCl <sub>2</sub>	20h	19
3	<b>1</b>	20h	Quantitative
4	<b>2</b>	20h	Quantitative
5	<b>3</b>	20h	Quantitative
6	<b>4</b>	20h	Quantitative
7	<b>5</b>	20h	Quantitative
8	<b>6</b>	20h	Quantitative

As shown in Table 4, zinc complexes **1-6** enhance the rate of the reaction for the reduction of pyridine-2-carboxaldehyde when compared to ZnCl<sub>2</sub>. Use of complexes **1-6** results in quantitative conversion of pyridine-2-carboxaldehyde to pyridin-2-ylmethanol.

As seen in Tables 3 and 4, enhancement for the reduction of 4-nitrobenzaldehyde or pyridine-2-carboxaldehyde was observed for complexes **1-6**. Stoichiometric conversion to the alcohol product was observed for pyridine-2-carboxaldehyde. Based on the mechanism proposed by Berreau and co-workers [36], the low activity of complexes **1-6** for the reduction of 4-nitrobenzaldehyde could be due to the slow hydrogen transfer between the co-factor and the substrate, which is coordinated to the zinc active site. More importantly, the alcohol product may inhibit the reaction. As the alcohol is formed, it may coordinate to the zinc metal center as the reaction progresses, and thereby hinder the reaction.

#### 4. Conclusions:

A series of Zn(II) compounds containing the SNS facial coordination of a tridentate pincer ligand were prepared and characterized. The tridentate SNS pincer ligand precursors and zinc complexes used in this work have provided new insights in the field of bioinorganic modeling chemistry. The zinc complexes serve as models for the zinc active site in liver alcohol dehydrogenase. The SNS zinc pincer complexes adopt a pseudo-tetrahedral geometry and have a SNS coordination environment about the zinc center like LADH and react with BNAH to reduce electron-poor aldehydes. The zinc complexes reported herein react with BNAH to quantitatively reduce pyridine-2-carboxaldehyde. The zinc complexes reported also reduce 4-nitro-benzaldehyde. It remains a challenge to synthesize a neutral zinc complex with a tridentate ligand with SNS donor atoms that yield reactivity that is comparable to LADH.

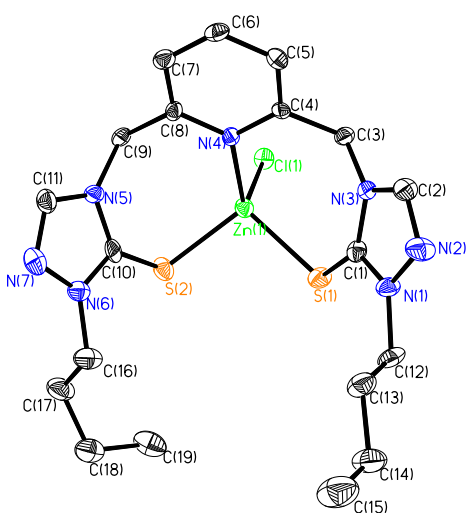
DFT calculations were performed to examine various structural and electronic properties of these compounds. The computed oxidation potentials match well with what is observed experimentally while the calculated reduction potential indicates that the experimental reduction wave does not correspond to a simple one-electron reduction of the ligand precursor without other reactivity occurring.

#### Supporting Information:

The  $^1\text{H}$ ,  $^{13}\text{C}$  and HSQC NMR spectra of **1a**, **2a**, **4a-6a**, **1b-6b**, and **1-6** and mass spectra of **1-6** are provided. IR spectra for **1b-6b** and crystallographic details of **1**, **3**, **5b**, and **6** are also given. The detailed descriptions for the syntheses of each compound are given as well.

### Graphical Abstract:

A series of tridentate SNS ligand precursors, based on bis-imidazole and bis-triazole precursors, were metallated with  $\text{ZnCl}_2$  to give new tridentate SNS pincer zinc complexes that serve as models for the zinc active site in Liver Alcohol Dehydrogenase (LADH). These systems were characterized with single crystal X-ray diffraction,  $^1\text{H}$ ,  $^{13}\text{C}$ , and HSQC NMR spectroscopies, and electrospray mass spectrometry, and were studied by density functional theory. The ability of these compounds to catalyze the reduction of electron-poor aldehydes was examined.



### Research Highlights:

- Synthesized and characterized a series of SNS Zn(II) pincer compounds
- Zn(II) complexes enhance reduction of aldehydes in presence of hydrogen donor
- Correlated cyclic voltammetry results with Gaussian calculations

**Acknowledgement:**

This work was supported by generous funding from The Fairfield University Science Institute (JRM), Fairfield University Start-up Funding (JRM), Fairfield University Research Grants (JRM), and an NTID Faculty Evaluation and Development Grant (MAL). JRM would like to thank Prof. Matthew A. Kubasik, and Prof. L. Kraig Steffen for helpful suggestions.

**5. References:**

- [1] R.H. Holm, P. Kennepohl, E.I. Solomon, *Chem. Rev.*, 1996, 96, 2239-2314.
- [2] J.A. Ibers, R.H. Holm, *Science*, 1980, 209, 223-235.
- [3] (a) W.N. Lipscomb, N. Sträter, *Chem. Rev.* 1996, 96, 2375-2433. (b) E. Kimura, T. Koike, M. Shionoya, *Structure and Bonding*, 1997, 89, 1-28.
- [4] K.K. Kannan, B. Nostrand, K. Fridborg, S. Lovgren, A. Ohlsson, M. Petef, *Proc. Natl. Acad. Sci, USA*, 1975, 72, 51.
- [5] A. Meibner, W. Haehnel, H. Vahrenkamp, *Chem. Eur. J*, 1997, 3, 261-267.
- [6] A. Dolega, *Coord. Chem. Rev.*, 2010, 254, 916-937.
- [7] A. Dolega, A. Pladzyk, K. Baranowska, J. Jezierska, *Inorg. Chim. Acta*, 2009, 362, 5085-5096.
- [8] L. Cronin, P.H. Walton, *Chem Commun*, 2003, 1572-1573.
- [9] L.M. Berreau, M.M. Makowska-Grzyska, A.M. Arif, *Inorg Chem*, 2001, 40, 2212-2213.
- [10] R.M. Kellogg, R.P. Hof, *J Chem Soc, Perkin Trans 1*, 1996, 1651-1657.
- [11] S.C. Shoner, K.J. Humphreys, D. Barnhart, J.A. Kovacs, *Inorg. Chem*, 1995, 34, 5933-5934.

[12] (a) B. Kaptein, G. Barf, R.M. Kellogg, F. Van Bolhuis, *J. Org. Chem*, 1990, 55, 1890-1891. (b) B. Kaptein, L.Wang-Griffen, G. Bart, R.M. Kellogg, *J Chem. Soc Chem Commun*, 1987, 1457-1459.

[13] D.T. Corwin, R. Fikar, S.A. Koch, *Inorg. Chem*, 1987, 26, 3079-3080.

[14] (a) C. Kimblin, T. Hascall, G. Parkin, *Inorg. Chem.*, 1997, 36, 5680-568. (b) C. Kimblin, B.M. Bridgewater, D.G. Churchill, G. Parkin, *Chem. Commun*; 1999, 2301-2302.

[15] (a) R. Walz, H. Vahrenkamp, *Inorg. Chim. Acta*, 2001, 314, 58-62. (b) Y.H. Zhang, H. Vahrenkamp, *Inorg. Chim. Acta*, 2003, 351, 201-206.

[16] (a) M. Albrecht, G. van Koten, *Angew. Chem. Int. Ed.*, 2001, 40, 3750-3781. (b) A.T. Normand, K.J. Cavell, *Eur. J. Inorg. Chem.*, 2008, 2781-2800.

[17] D. Morales-Morales, C.M. Jensen, eds. *The Chemistry of Pincer Compounds*, Elsevier: New York, 2007.

[18] (a) C. Kimblin, T. Hascall, G. Parkin, *Inorg. Chem.*, 1997, 36, 5680-568. (b) C. Kimblin, B.M. Bridgewater, D.G. Churchill, G. Parkin, *Chem. Commu*, 1999, 2301-2302. (c) C. Bergquist, G. Parkin, *Inorg. Chem.*, 1999, 38, 422-423. (d) G. Parkin, *Chem. Rev*, 2004, 104, 699-767. (e) B.M. Bridgewater, T. Fillebeen, R.A. Friesner, G. Parkin, *J. Chem. Soc., Dalton Trans*, 2000, 4494-4496. (f) J.G. Melnick, A. Docrat, G. Parkin, *Chem. Commun*, 2004, 2870-2871. (g) C. Kimblin, B.M. Bridgewater, D.G. Churchill, T. Hascall, G. Parkin, *Inorg. Chem*, 2000, 39, 4240-4243.

[19] (a) M. Tessmer, M. Shu, H. Vahrenkamp, *Inorg. Chem.*, 2001, 40, 4022-4029. (b) J. Seebacher, M. Shu, H. Vahrenkamp, *Chem. Commun*; 2001, 1026-1027. (c) Y.H. Zhang, H. Vahrenkamp, *Inorg. Chim. Acta*, 2003, 351, 201-206. (d) M.M. Ibrahim, M. Shu, H. Vahrenkamp, *Eur. J. Inorg. Chem*, 2005, 1388-1397. (e) R. Walz, H. Vahrenkamp, *Inorg. Chim. Acta*, 2001, 314, 58-62. (f) M. Rombach, J. Seebacher, M. Ji, G. Zhang, G. He, M. Ibrahim, B. Benkmil, H. Vahrenkamp, *Inorg. Chem*, 2006, 45, 4571-4575. (g) M. Ibrahim, J. Seebacher, G. Steinfeld, H. Vahrenkamp, *Inorg. Chem*, 2005, 44, 8531-8538.

[20] J.R. Miecznikowski, W. Lo, M.A. Lynn, B.E. O'Loughlin, A. P. DiMarzio, A. M. Martinez, L. Lampe, K. M. Foley, L. C. Keilich, G. P. Lisi, D. J. Kwiecien, C. M Pires, W. J. Kelly, N. F. Kloczko, K. N. Morio, *Inorg. Chim. Acta*, 2011, 376, 515-524.

[21] J.A. Loch, M. Albrecht, E. Peris, J. Mata, J.W. Faller, R. H. Crabtree. *Organomet*, 2002, 21, 700-706.

[22] J.R. Miecznikowski, R.H. Crabtree. *Polyhedron*, 2004, 23, 2857-2872; (b) J.R. Miecznikowski, R.H. Crabtree, *R.H. Organomet*, 2004, 23, 629-631.

- [23] J.B. Polya, A. J. Blackman. *J. Chem. Soc. C.*, 1971, 1016-1018.
- [24] A.A. Gridnev, I.M. Mihaltseva. *Synth. Commun.*, 1994, 24, 1547.
- [25] M. Albrecht, J.R. Miecznikowski, A. Samuel, J.W. Faller, R.H. Crabtree, *Organomet*, 2002, 21(17), 3596-3604.
- [26] C. Ainsworth, N.R. Easton, M. Livezey, D.E. Morrison, W.R. Gibson. *J. Med Pharm. Chem*, 1962, 5, 383-389.
- [27] P. G. Bulger, I. F. Cottrell, C. J. Cowden, A.J. Davies, U-H Dolling. *Tet Lett*, 2000, 41, 1297-1301.
- [28] J. Lutz, F. Hollmann, T.V. Ho, A. Schnyder, R. Fish, A. Schmid, *J. Organomet. Chem*, 2004, 689, 4783-4790.
- [29] APEX II, v2009, 3.0; Bruker AXS: Madison, WI 2009.
- [30] Sheldrick, G.M. *Acta Crystallogr.*, 2009, A64, 112-122.
- [31] M.J. Frisch, G.W. Trucks, H.B. Schlegel, G.E. Scuseria, M.A. Robb, J.R. Cheeseman, J. A. Montgomery Jr., T. Vreven, K.N. Kudin, J.C. Burant, J. M. Millam, S. S. Iyengar, J. Tomasi, V. Barone, B. Mennucci, M. Cossi, G. Scalmani, N. Rega, G.A. Petersson, H. Nakatsuji, M. Hada, M. Ehara, K. Toyota, R. Fukuda, J. Hasegawa, M. Ishida, T. Nakajima, Y. Honda, O. Kitao, H. Nakai, M. Klene, X. Li, J.E. Knox, H.P. Hratchian, J.B. Cross, V. Bakken, C. Adamo, J. Jaramillo, R. Gomperts, R.E. Stratmann, O. Yazyev, A.J. Austin, R. Cammi, C. Pomelli, J.W. Ochterski, P.Y. Ayala, K. Morokuma, G.A. Voth, P. Salvador, J.J. Dannenberg, V.G. Zakrzewski, S. Dapprich, A.D. Daniels, M.C. Strain, O. Farkas, D.K. Malick, A.D. Rabuck, K. Raghavachari, J.B. Foresman, J. V. Ortiz, Q. Cui, A.G. Baboul, S. Clifford, J. Cioslowski, B. B. Stefanov, G. Liu, A. Liashenko, P. Piskorz, I. Komaromi, R.L. Martin, D.J. Fox, T. Keith, M.A. Al-Laham, C.Y. Peng, A. Nanayakkara, M. Challacombe, P.M.W. Gill, B. Johnson, W. Chen, M.W. Wong, C. Gonzalez, J.A. Pople, *Gaussian 03, Revision E.01*; Gaussian, Inc.: Wallingford, CT, 2004.
- [32] (a) W.R. Fawcett, *Langmuir*, 2008, 24, 9868. (b) L.E. Roy, E. Jakubikova, G. Guthrie, E.R. Batista, *J. Phys. Chem. A*, 2009, 113, 6745-6750.
- [33] S. Al-Karadaghi, E.S. Cedergren-Zeppezauer, S. Hövmoller, K. Petratos, H. Terry, K.S. Wilson. *Acta Cryst*, 1994, D50, 793-807
- [34] B.V. Trzhtsinskaya, N.D. Abramova, *J Sulfur Chemistry*, 1991, 10(4), 389-421.
- [35] A. Suszka, *Polish J. Chem*, 1980, 54, 2289-2295.

[36] M.M. Makowska-Grzyska, P.C. Jeppson, R.A. Allred, A.M. Arif, L.M. Berreau. *Inorg. Chem*, 2002, 41, 4872-4887.